CHAPTER-5

MINERALOGY

"God sleeps in the minerals, awakens in plants, walks in animals, and thinks in man."
Arthur Young

5.1 Introduction

This chapter presents the mineral chemistry of high-grade gneisses and granulites. An attempt has been made to decode the history of formation of high-grade gneiss and granulites of the study area as they provide valuable information on understanding the deep crustal processes. The various rock types from Daltonganj of the Chhotanagpur Granite Gneiss Complex (CGGC) show diverse mineral assemblages, which are obtained from their detailed petrographic studies (see chapter 4).

Electron microprobe analyses (EPMA) of various silicate minerals have been carried out for selected rock samples of the study area. Wherever possible, an attempt has been made to correlate mineral chemistry with the host rock's bulk composition. Special attention has been paid to record any chemical zoning present in the minerals during the electron microprobe analyses. The EPMA has been carried out for fresh minerals (avoiding altered minerals). The emphasis has been given to analyses of coexisting mineral phases suitable for geothermometry (models applicable to; garnet-clinopyroxene, garnet-orthopyroxene, clinopyroxene-orthopyroxene, garnet-cordierite, garnet-biotite) and geobarometry (garnet-cordierite-sillimanite-quartz and garnet-clinopyroxene-plagioclase-quartz). Geothermometers are generally based on cations' exchange, especially Fe-Mg between the coexisting minerals. Therefore, geothermometers are

sensitive to Fe-Mg re-equilibrations and often calculate temperature at the time of crystallization of mineral.

On the other hand, geobarometers rely mostly on the net transfer reactions, especially at high temperatures and are less sensitive to late ion re-equilibrations. [280] have demonstrated that more accurate and realistic peak temperatures-pressures could be estimated by studying relict mineral assemblages in rock types. The analyzed sample's location is shown in the geological map of the area (Fig.3.3). Prior to the discussion of mineralogy, the analytical method used to analyses the rocks and the minerals are discussed below.

5.2 EPMA analytical technique

The analytical work was carried out on the EPMA (CAMECA SX Five) instrument at DST–SERB National Facility, Department of Geology, Centre of Advanced Study, Institute of Science, Banaras Hindu University. A polished thin section was coated with 20 nm thin layer of carbon by using the LEICA-EM ACE200 instrument. The CAMECA SX Five instrument was operated at a voltage of 15 kV and current 10 nA with a LaB6 source in the electron gun for the electron beam generation. Natural silicate mineral andradite as an internal standard was used to verify positions of crystals (SP1-TAP, SP2-LiF, SP3-LPET, SP4-TAP and SP5-PC1) concerning the corresponding wavelength dispersive (WD) spectrometers (SP#) in CAMECA SX Five instrument. The following X-ray lines were used in the analyses: F-Kα, Na-Kα, Mg-Kα, Al-Kα, Si-Kα, P-Kα, K-Kα, Cl-Kα, Ca-Kα, Ti-Kα, Cr-Kα, Mn- Kα, Fe-Kα, Ni-Kα and Sr-Lα. Natural mineral standards: apatite, albite, halite, periclase, peridotite, corundum, wollastonite, orthoclase, rutile, chromite, rhodonite, celestite, barite, hematite and

synthetic Ni metal supplied by CAMECA AMETEK were used for routine calibration and quantification. Routine calibration, acquisition, quantification and data processing were carried out using SxSAB version 6.1 and SX-Results software of CAMECA. The representative EPMA data of different minerals are presented in Tables 5.1–5.11.

5.3 Garnet

Garnet constitutes the leading mineral group in the metamorphic rocks, which is essential to interpret the metamorphic rocks' genesis. Garnet from different rock types essentially consists of a solid solution of almandine, pyrope, grossularite, and spessartine end members. Garnets have proved a wide range in chemical composition which depends on the mineral assemblage, bulk rock chemistry and metamorphic condition. The microprobe analyses and the structural formulae based on 12 oxygen atom of garnet from the high-grade gneiss, pelitic granulite and mafic granulite are presented in Table 5.1.

The garnets' stoichiometry corresponds closely to the ideal formula: **$(Fe^{2+}$,Mg, Mn, Ca)$_3$ (Al, Ti, Cr, $Fe^{3+})_2$ Si_3O_{12}**, there is a minor deficiency in the sum of the divalent cations. The structural formulae of the garnet are $X_3Y_2Z_3O_{12}$ (on 12 oxygen basis), where, X is an 8 coordinated site that includes $(Fe^{2+}$, Mn, Mg, Ca$)_3$, Y is a 6-coordinated site that includes (Al, Ti, Cr, $Fe^{3+})_2$ and Z is a tetrahedral site that generally includes (Si_3O_{12}). The garnets consist of 42.15 to 79.93 mole % almandine, 13.27 to 30.72 mole % pyrope, 0.69 to 18.65 mole%, grossularite and 0.45 to 25.77 mole% spessartite end members in the studied rocks. Pyrope contents of garnet from the different rock types indicate the following trend: high-grade gneisses > pelitic granulites > mafic granulites. Whereas the grossularite contents of garnet show reverse trend: Mafic granulites > pelitic granulites > high-grade gneisses. The analyzed garnets are plotted in (Ca+Mn)–Mg–Fe^{2+} diagram

(Fig.5.1a). All the garnet plots from the high-grade gneisses and pelitic granulites fall in the almandine- pyrope region, whereas the plot of the garnets from the mafic granulites shows higher contents of grossularite- spessartite. The Mn-rich garnets are described mostly from the hornfels [281] with MnO content of up to 12 wt%. The X_{Mg} in the garnets from Daltonganj varies from 0.17–0.31. This range may be attributed to Mn or Ca, which occupy the eight-fold coordination site in the garnet's crystal structure. The X_{Mg} vs Ca/Mn plots do not show any distinct correlation (Fig.5.1b).

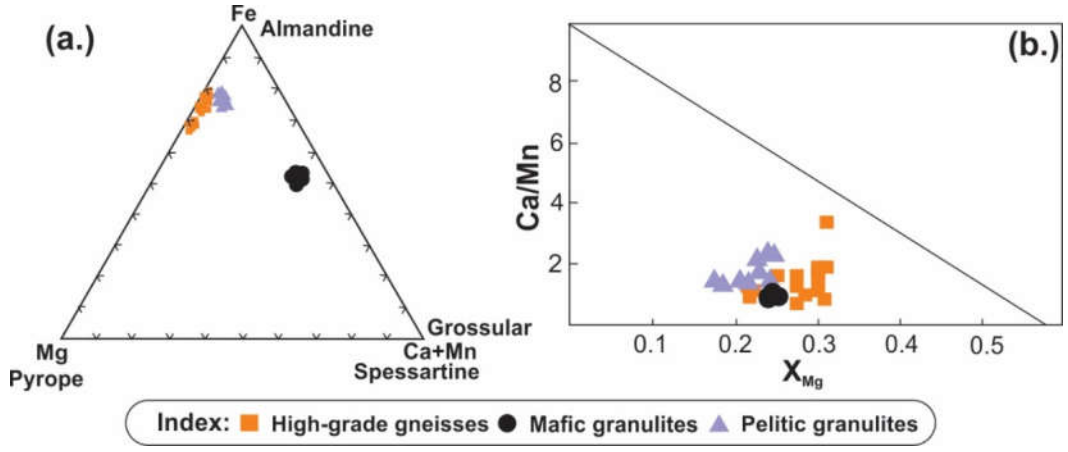

Figure 5.1(a) Triangular diagram showing the variation in (spessartine + grossular)–almandine–pyrope end member compositions in the garnets from different rock types. (b) A plot of X_{Mg} vs Ca/Mn of garnets, from different rock types.

5.3.1 Garnet zoning

Garnets are zoned with X_{Mg} in the cores compared to the rim. Biotite's inclusions are observed in garnet porphyroblast, X_{Mg} in garnet decreases abruptly near the inclusions. The BSE image from high-grade gneiss shows the inclusion of biotite and quartz in garnet (Fig.5.2a), and the elemental X-ray map of garnet reveals the enrichment of Fe and Mg elements (Fig.5.2b&c) and depletion of Mn and Ca elements (Fig.5.2d&e). The compositional variation in garnet is controlled by solid solution between four end members and thus their compositional variation can be described in terms of the

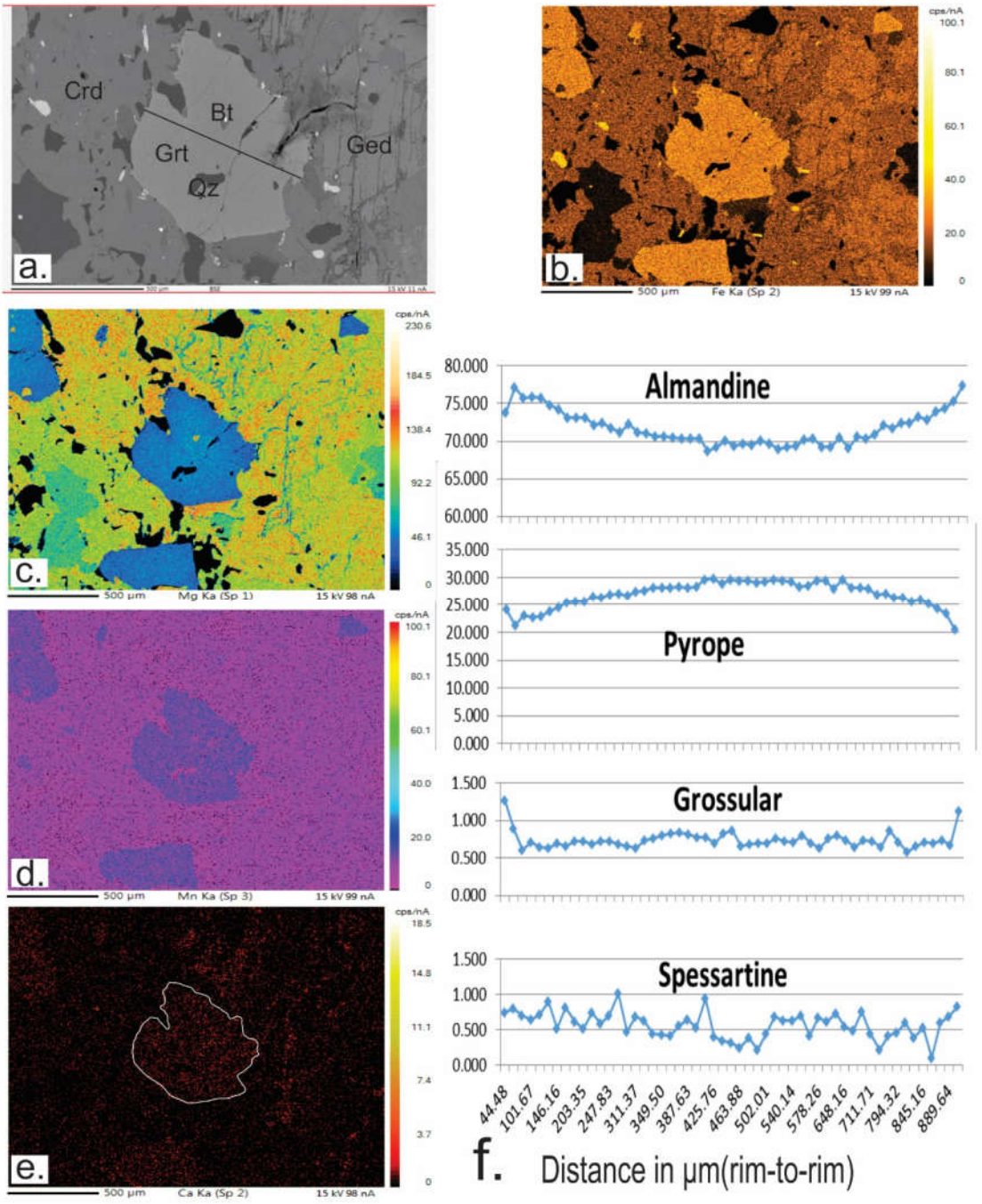

Figure 5.2 (a) BSE image of garnet porphyroblast with inclusions of biotite and quartz; (b–e) these images represent the X-ray mapping of Fe, Mg, Mn and Ca in garnet porphyroblast; (f) X_{Alm}, X_{Py}, X_{Grs} and X_{Sps} variation along the garnet porphyroblast from rim to rim.

independent variables of the four end members. Garnet shows the almandine dominance in which X_{Alm} varies from 0.68 to 0.77. The porphyroblastic garnet's length is 890 µm,

and the rim–core–rim distribution of almandine and pyrope garnet is graphically represented (Fig.5.2f). Here almandine shows a high-composition peak at the rim and a lower one at the core area. Pyrope represents a higher occurrence at the core and lowers occurrence at the rim portion (X_{Py} = 0.22–0.34). The Fe content of garnet increases and the Mg content decreases at the rim of the garnet porphyroblast due to locally resorbed by gedrite + cordierite minerals or by retrogressive biotite. This situation indicates the lowering of the pressure and the temperature at the rim of garnet porphyroblast compared to the core portion. This is in contrary to other areas, where prograde zoning in granulites has been studied [282], with the increasing temperature up to 600–700°C and increase rate of intracrystalline diffusion led to the reduction of existing chemical profiles, thereby homogenizing growth zonation [283-285].

5.3.2 Ca & Mn content of garnet

CaO-contents of the garnets are low with 0.239 to 6.936 mol% of grossularite. The highest limit is observed in the garnets from the mafic granulites and least ones in garnets from the high-grade gneisses and pelitic granulites. Mn-content of garnets shows wide range (0.014–0.816 p.f.u). The upper limit is found in the mafic granulites.

5.4 Amphibole

The word “amphibole” is derived from a Greek word introduced by [286], which means an allusion of the mineral having various composition and appearance. The amphibole and pyroxene groups of minerals are chain silicates, the initial work of which was described by [287]. In 1961 Schaller, recognized the essential constituents of amphibole group mineral, making it different from pyroxene in an abundance of hydroxyl ions.

Amphibole is made up of $(Si,Al)O_4$ tetrahedral silicate linked to form a double chain and has a unit composition of Si_4O_{11}. The double chain silicates have two tetrahedral which lie at the inner and outer part of each chain T1 and T2 respectively, which repeated along C-axis of an unit cell at an interval of approximately 5.3Å. A hexagonal shape space is formed through double chain silicate, which is usually linked by hydroxyl ion.

The general formula of amphibole is $\mathbf{A_{0\text{-}1}B_2C_5T_8O_{22}(OH,F)_2}$; where, **A-site** is for large cation Na, K; **B-site** for the cation at M4 site Ca, Na; **C-site** for cation at M1, M2, M3 (usually medium size cation) sites; **T-site** those in tetrahedral T1 and T2 coordinated by O_3 (OH) in an octahedral manner.

5.4.1 Classification of amphibole

The group and nomenclature of amphiboles from the high-grade gneiss and mafic granulites have been assigned based on Ca+Na vs Na diagram [288] that suggest magnesium-iron-manganese amphibole (gedrite) present in high-grade gneiss and calcic-amphibole (hornblende) present in mafic granulites.

5.4.2 Hornblende

The microprobe analyses of hornblende from mafic granulites are presented in Table 5.2 along with their structural formula calculated based on 23 oxygen atoms. The structural formulae of the analyzed hornblende correspond to the general formula of calcic amphibole $\mathbf{[(Ca, Na, K)_{2\text{-}3}(Mg, Fe, Cr, Mn, Al^{VI}, Ti)_5 (Si, Al^{IV})_8 O_{22} (OH)_2]}$.

The Alumina content of hornblende is dependent on (a) host rock composition particularly $Al_2O_3/(Al_2O_3 + SiO_2)$ ratio (b) PT conditions [289] proposed that the Al^{IV}-content of hornblende increases with pressure, the hornblende from magmatic and

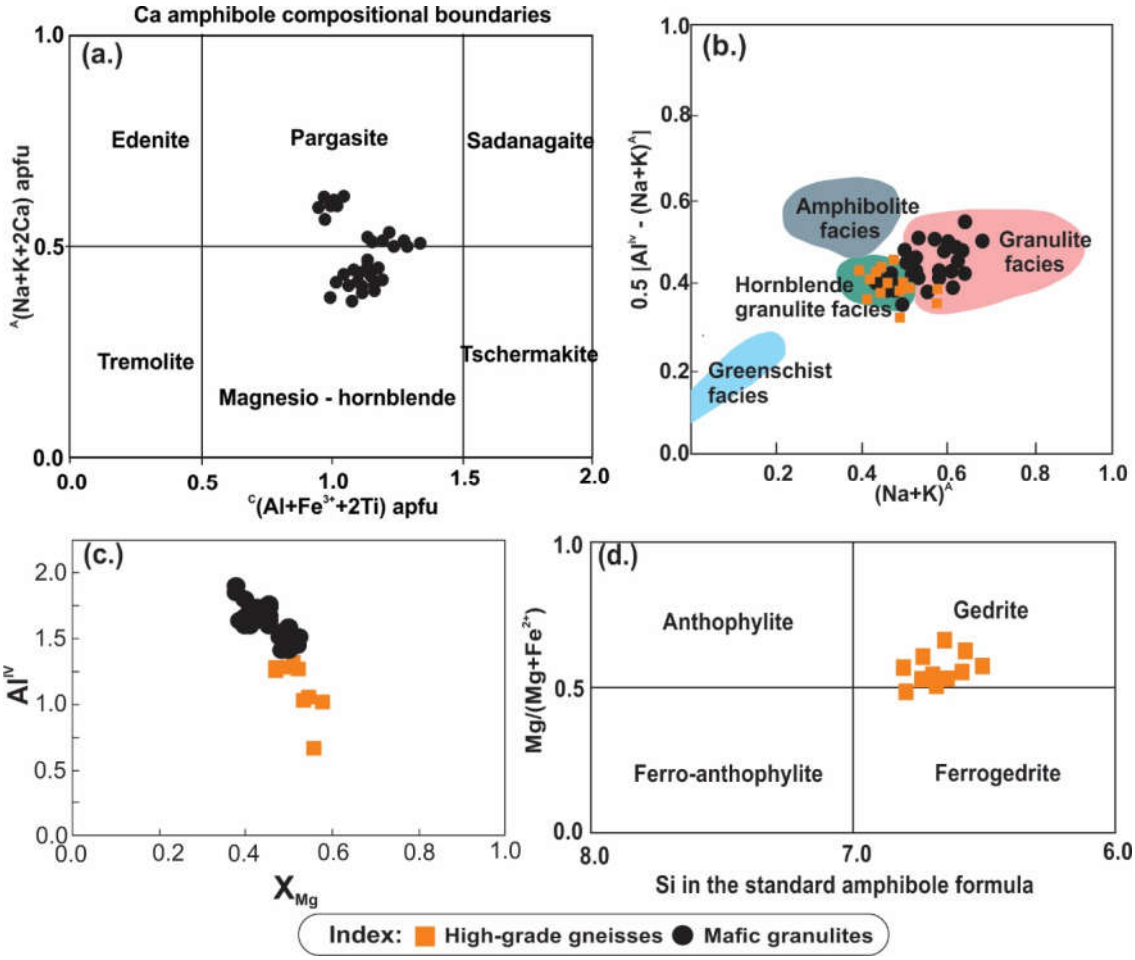

Figure 5.3(a) Amphibole classification diagram (after [290]) for the Daltonganj mafic granulites. (b) Plot $0.5[Al^{IV}–(Na+K)^{A}]$ vs $(Na+K)^{A}$ a.p.f.u for calcic amphibole from greenschist to granulite facies (after [291]) expressed as Daltonganj mafic granulite belongs to granulite facies rock. (c) A plot of X_{Mg} vs Al^{IV} of garnets, from different rock types. (d) Leaks classification diagram for the amphiboles.

contact metamorphic rocks generally have lower Al^{VI} and Si contents than hornblende in regionally metamorphosed rocks. The Al^{IV} and Al^{VI} content of hornblende varies from 1.453 to 1.875 and 0.0 to 0.478 p.f.u. respectively. According to the International Mineralogical Association (IMA) association recommendation [290], they are classified as Pargasite and Magnesio- hornblende (Fig.5.3a). The chemical composition of hornblende is expressed in $0.5[Al^{vi}–(Na+K)^{A}]$ vs $(Na+K)^{A}$ plot (Fig.5.3b) [291]. The X_{Mg} ratio of hornblende ranges from 0.38 to 0.52. The hornblende's structural formulae

clearly show a decrease of X_{Mg} with an increase of Al^{IV}-content (Fig.5.3c). The hornblende from the Daltonganj region contain (p.f.u) Na = 0.260–0.413, K = 0.158–0.352 and Ti = 0.145–0.276. This indicates that these hornblendes have crystallized near the metamorphism's thermal peak under granulite facies.

5.4.3 Gedrite

The microprobe analyses and the gedrite's structural formulae based on 23 Oxygen are presented in Table 5.3. The analyzed amphiboles have (Ca + Na) < 1.0; (Mg, Fe^{2+}, Mn, Li) ≥1.0 and Li-poor and therefore, these are Mg–Fe–Mn–Li amphiboles according to [292] classification. However, analyzed data plotted on Leaks classification diagram (Fig.5.3d) then all the plots fall in the gedrite field, and the structural formulae of gedrite is [$\mathbf{Na_{0.5}\ (Mg,\ Fe^{2+})_2\ (Mg,Fe^{2+})_{3.5}\ Al_{1.5}Si_6Al_2O_{22}(OH)}$]. In this granulitic rock, gedrite has fluorine content which varies from 0.19 to 0.46 wt%. Al^{IV} and Al^{VI} are present in a sufficient amount of 0.64–1.35 and 0.47–0.83 p.f.u., respectively. The X_{Mg} ranges from 0.54 - 0.60. Gedrite contains significant amounts of Na_2O varies from 0.793–1.82 Wt%.

5.5 Pyroxene

The name *pyroxene* is derived from the Greek world, which was first introduced by [286]. *Pyroxene* is a combination of two words: which mean pyro-*fire* and xenos-*stranger*. It is an anhydrous single-chain silicate mineral found in both igneous and metamorphic rock. Four components: $CaMgSi_2O_6$-$CaFeSi_2O_6$-$Mg_2Si_2O_6$-$Fe_2Si_2O_6$ (Diopside-Hedenbergite-Enstatite-Ferrosilite) based nomenclatures of pyroxenes were first described by [293]. Later, IMA/CNMMN (International Mineralogical Association/ Commission on New Minerals and Mineral Names; [294] and references therein) provided a series of recommendations and schemes for the classification nomenclature of

pyroxenes. This nomenclature was later modified by [295]. The first pyroxene (diopside) structure was determined by [296]. They established that the pyroxene structure is linked by SiO_4 tetrahedral by sharing two oxygen atoms out of four by each tetrahedron, forming a single chain structure.

Cations laterally surround this chain in M1 and M2 sites. M1 site atom lies between the apices and M2 site at the base of SiO_3 tetrahedral chain. Further pyroxene can be sub-grouped based on cation participation in M1 and M2 sites, mostly depending on variable parameters such as P and T. The co-ordination of oxygen at M1 site is fixed, i.e. octahedral whereas at M2 site, it is variable according to the cation size, for instance, Mg in six-fold coordination; eight fold coordination for Na- Ca. The microprobe analysis and structural formulae (calculated based on 6 oxygen) of orthopyroxene and clinopyroxene are presented in Tables 5.4 and 5.5, respectively. The recalculated formulae approximate to the ideal formula: [$\mathbf{(Mg, Fe^{2+}, Al, Ti, Mn, Ca)_2\ (Si, Al)_2\ O_6}$].

5.5.1 Orthopyroxene

The analyzed pyroxene are plotted in a triangular end members $CaSiO_3$–$MgSiO_3$–$Fe^{2+}SiO_3$ diagram (Fig.5.4) The orthopyroxene plot of high-grade gneisses and mafic granulites lies at $En_{39\text{-}58}$ near the hypersthene which is the solid solution between Mg and Fe end members of the orthopyroxene. An essential feature of orthopyroxene chemistry is the Al content this may be dependent on several factors: (a) Host rock composition, (b) the composition of the coexisting mineral [297-299], (c) the pressure-temperature conditions of formation [300]. The Al of the orthopyroxene varies between 0.01–0.169 p.f.u. The X_{Mg} ranges between 0.39 and 0.63 and corresponds to hypersthene. The Ca-content of orthopyroxene (0.0 to 0.04 p.f.u) based on 6 oxygen, is lower than the cpx.

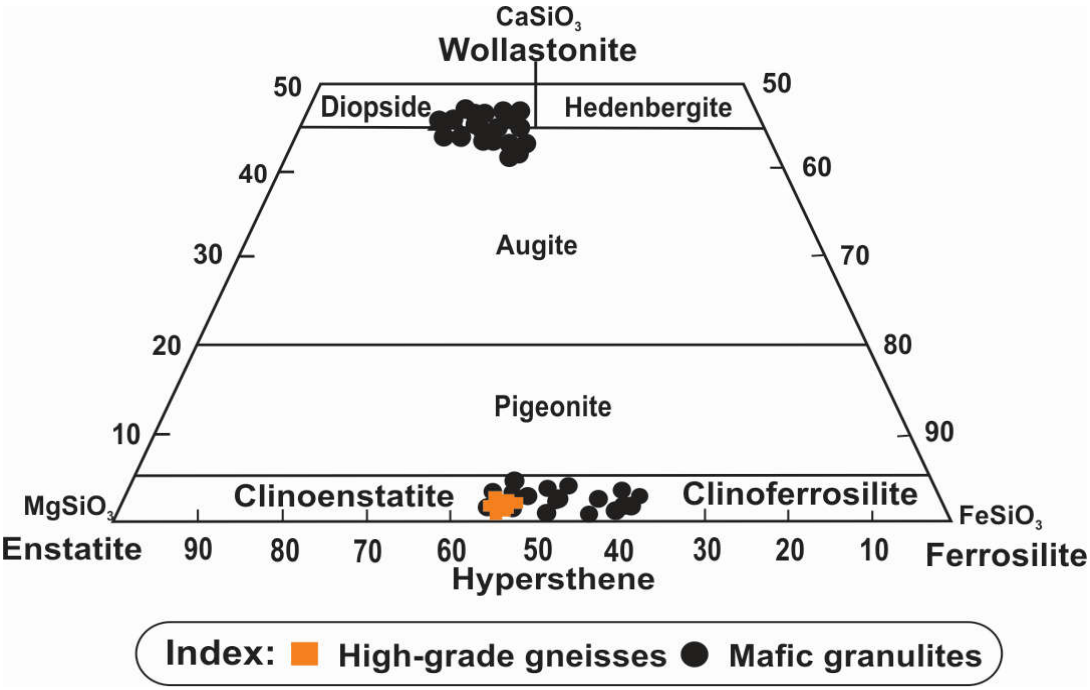

Figure 5.4 A $CaSiO_3$- $MgSiO_3$- $FeSiO_3$ composition diagram of proroxenes showing the plot of ortho and clinopyroxenes from different rock types.

5.5.2 Clinopyroxene

The coexisting clinopyroxene plot in a triangular end member $CaSiO_3$–$MgSiO_3$ – $Fe^{2+}SiO_3$ diagram lies in the field of augite and diopside. The X_{Mg} of clinopyroxene ranges between 0.45 and 0.63. It has higher X_{Mg} and Al-content compared to orthopyroxene. Ca-content of the clinopyroxene varies between (0.491 to 0.908 p.f.u) suggest the evidence of high content of Ca in clinopyroxene, which is a characteristic of mafic granulite assemblages. The Al_2O_3 content in clinopyroxene varies between 0.55 to 1.66 wt%. The higher amounts of Al_2O_3 present reflect an increasing Jadeite component, indicating higher pressures attained during metamorphism.

5.6 Cordierite

Cordierite is a magnesium-iron-aluminium cyclo-silicate that occurs in contact or regional metamorphism of argillaceous rocks. The stoichiometry approximates to the

ideal formula: [(Mg, Fe^{2+})$_2$ ($Al_4Si_5O_{18}$)**n**H_2O]. Iron in the cordierite is almost always present, and a solid solution exists between Mg-rich and Fe-rich cordierite. Cordierite structure accommodates molecular water with values of **n** commonly between 0.15 and 0.80 [301]. The cordierite analyses show summation between 94.035 to 99.053 wt%, suggesting that it may be hydrous containing 0.947–5.965 wt% H_2O and gaseous species as cordierite contains a large channel site at the center of its six-members ring structure that can accommodate molecular H_2O, CO_2 and to a lesser extent other volatile species such as CH_4, N_2 and Ar [302-307]. It is now well accepted that cordierite's molecular water content is a function of P and T [308-310]. The analyses of cordierite with their structural formulae based on 18 Oxygen from high-grade gneisses and pelitic granulite are listed in Table 5.6.

The X_{Mg} varies between 0.63 and 0.79. Higher values correspond to the cordierite from the high-grade gneisses (0.74–0.79) as a comparison to the pelitic granulites (0.63–0.69). The microprobe studies of the cordierite indicate only limited and irregular zoning, reflecting variable dominance of the effect of small scale cation exchange with inclusion, diffusion and continuous re-equilibration with matrix grains following nucleation. Insignificant amounts of Na_2O and K_2O are commonly present, range from 0.094 to 0.314 wt% and 0.0 to 0.022 wt%, respectively. [311] suggested that K contents increases with temperature and decreases with water content. Thus, it can be inferred that water content in cordierite will below based on the depletion of K in cordierite.

5.7 Mica

The mica minerals belong to phyllosilicate commonly found in igneous, metamorphic and sedimentary rocks. It is mainly composed of two sheets silicon

tetrahedral between which octahedrally coordinated cation exists. Additional OH^- (hydroxyl ion) is associated and completes the sandwiched octahedral cations. These octahedral cations coordination are either in the form of *brucite layer* $Mg_3(OH)_6$ or in *gibbsite layer* $Al_2(OH)_6$. The general chemical formula of micas is $\mathbf{X_2Y_{4\text{-}6}Z_8O_{20}(OH,F)_4}$ where; **X** is for K, Na, Ca, Ba, Rb, Cs; **Y** is for Al, Mg or Fe, Mn, Cr, Li and **Z** is for Si or Al but also for Fe^{3+} and Ti^{4+}.

The Mica group is further subdivided based on several Y ions present is 4 and 6 dioctahedral (muscovite) and tri-octahedral (biotite) classes. However, mica can be sub-classified as *common mica* in which K or Na are dominant ions in X, whereas if Ca ion is present, then it is known as *brittle mica*. In trioctahedral mica, the number of Y ions equals 3 atoms. Depending upon prevailing Physico-chemical conditions and nature of melt, sometimes K in the X site may be replaced by Ba, Rb or Cs and, therefore, a total sum of X site in the formula may be more than unity.

5.7.1 Biotite

The analytical electron microprobe data of biotite from high-grade gneisses and granulites, with their structural formula (calculated on the basis of 22 oxygen) are presented in (Table 5.7). The structural formula approximated to the ideal formula of biotite: $\mathbf{[(K,Na,Ca)\ (Al^{VI},\ Mg,\ Fe,\ Mn,\ Ti)_3\ (Si,\ Al^{IV})_4\ O_{10}\ (OH)_2]_2}$.

The biotite exhibits composition between the end members annite $[K_2Fe_6(Si_6Al_2O_{20})(OH)_4]$, siderophyllite $[K_2Fe_5Al(Si_5Al_3O_{20})(OH)_4]$, phlogopite $K_2Mg_6(Si_6Al_2O_{20})(OH)_4]$, eastonite $[K_2Mg_5Al(Si_5Al_3O_{20})(OH)_4]$. The biotites' analyses display a wide range of X_{Mg} (0.46 to 0.74). The wide range of variation indicates the following trend of X_{Mg} in biotites; high-grade gneisses (0.71 to 0.74) > pelitic granulites

(0.58 to 0.61) > mafic granulites (0.46 to 0.54). The Al^{IV} content of all studied rock samples varies from 2.22 to 2.508 p.f.u.

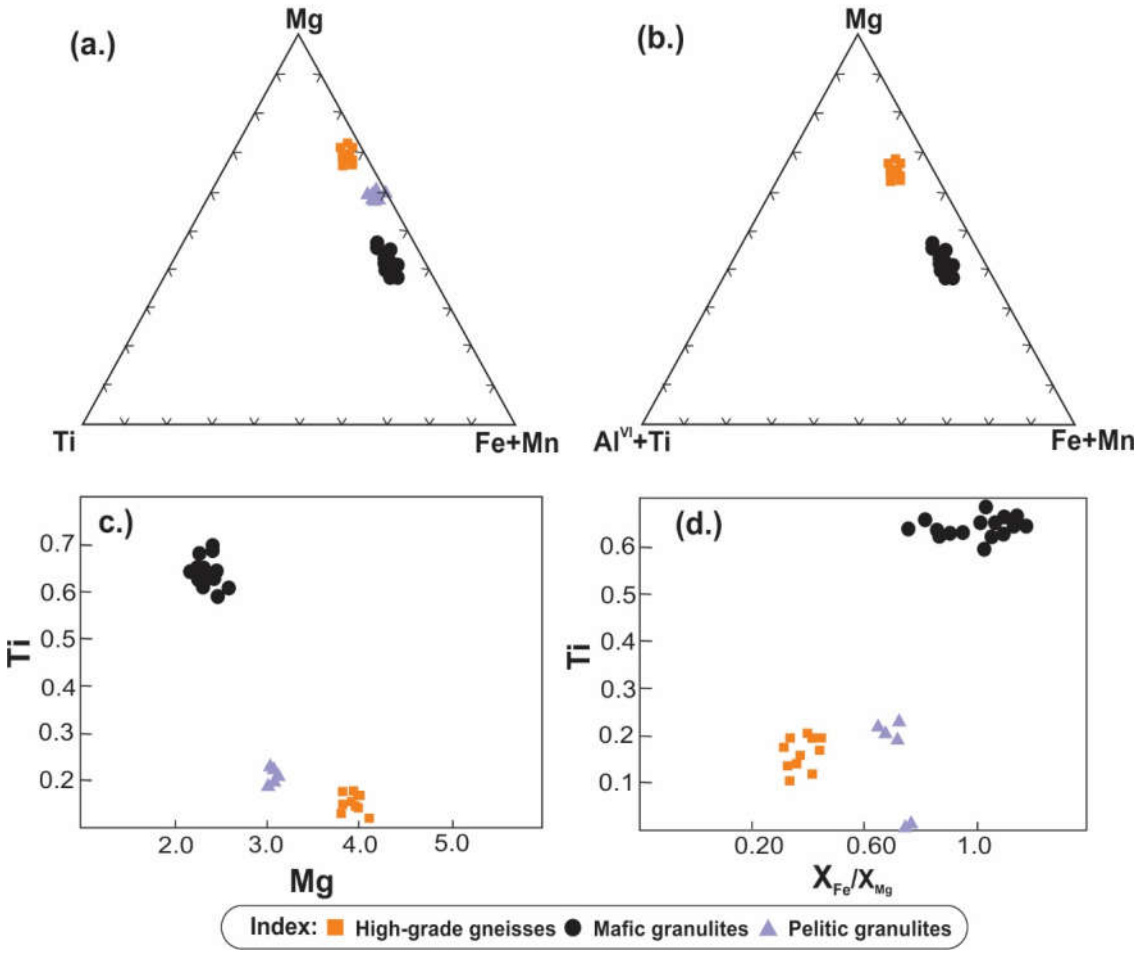

Figure 5.5 (a) A plot of microprobe analyses of biotites from different rock type in Mg- Ti -(Fe+Mn) diagram. (b) A plot of microprobe analyses of biotites from different rock type in Mg-(Al^{IV}+Ti) - (Fe+Mn) diagram. (c) A plot of Ti vs Mg showing negative trend. (d) A plot of X_{Fe}/X_{Mg} vs TiO_2 showing linear relationship.

In triangular diagram Mg–(Fe+Mn)–Ti (Fig.5.5a), the plot of biotite is lying between Mg and (Fe+Mg) line. The plot of biotites from different rocks shows a decrease of Ti with an increase of Mg, suggesting preferential substitution of Mg by Ti in the octahedral layer. In Mg–(Fe+Mn)–(Al^{IV}+Ti) (Fig.5.5b), a plot of biotite depicts the

decrease of (Al^{IV}+Ti) with an increase in Mg, indicating that Al^{VI}+Ti substitutes Mg relative to Fe.

5.7.1.1 TiO_2 content

TiO_2 content of biotite is very significant in estimating the rock's metamorphic grade [312-314]. In the Daltonganj region's analyzed biotites, the amount of TiO_2 in biotite from the mafic granulite is higher than pelitic granulite and high-grade gneisses. TiO_2 contents of biotite from high-grade gneisses range from 1.14–2.08 wt% and in pelitic granulites 1.55–1.99 wt%. The high content of (more than 5 wt%) TiO_2 in biotite from mafic granulite, although the low content of TiO_2 in various rocks may be due to their formation was observed during retrogression. The plots of Ti vs Mg (Fig.5.5c) and Ti vs X_{Fe}/X_{Mg} (Fig.5.5d) show a negative and linear correlation, respectively.

5.8 Feldspar

The original name of feldspar was *feldtspat* which refers to the presence of the spar (spath) in tilled field (Swedish; feldt or falt) overlying granite, rather than German 'Fels' meaning rock. The feldspar group of minerals is ubiquitous in most of the studied lithounits. Indeed feldspar is termed as quaternary feldspar because of inclusion of celsian (Ba-feldspar) in additional to common end-members orthoclase (Or)-albite (Ab)-anorthite (An). Feldspars can be considered as two distinct binary solutions: the alkali feldspars $NaAlSi_3O_8$–$KAlSi_3O_8$ (albite-orthoclase) and the plagioclase feldspars $NaAlSi_3O_8$–$CaAl_2Si_2O_8$ (albite-anorthite). Feldspars from different rock types are plotted in the triangular $NaAlSi_3O_8$–$KAlSi_3O_8$–$CaAl_2Si_2O_8$ diagram (Fig.5.6).

The representative microprobe analyses and structural formulae of plagioclase and K-feldspar (calculated on the basis of 32 Oxygen) are shown in Table 5.8. The X_{Ca} =

[Ca/(Na+Ca+K)] ratio of pelitic granulite range from 37.84 to 38.67 (i.e andesine) and 41.31 to 67.85 (i.e labradorite to bytownite) in mafic granulite. The plagioclase is unzoned. The recalculation of the general formula of plagioclase $(Ca, Na, K)_2(Al, Si)_8O_{16}$

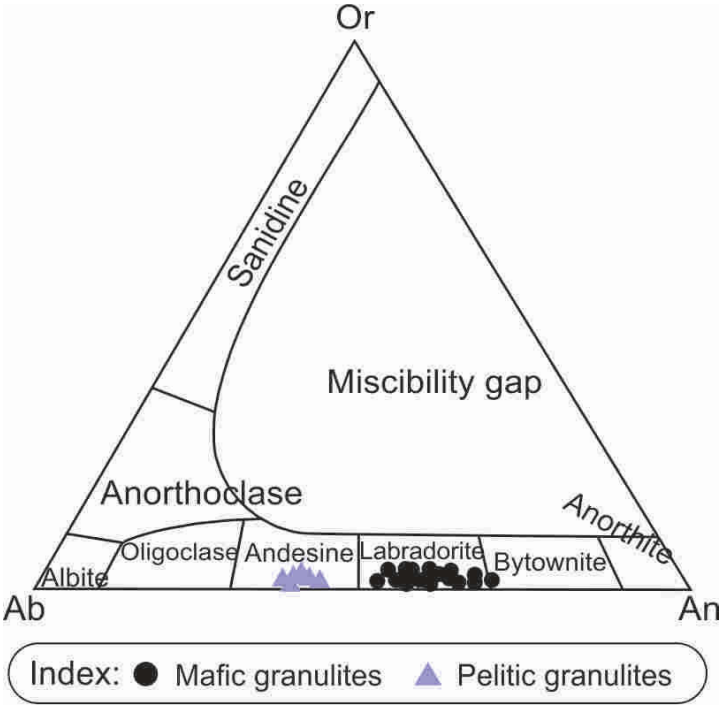

Figure 5.6 Triangular $NaAlSi_3O_8$–$KalSi_3O_8$–$CaAl_2Si_2O_8$ diagram showing plots of alkali feldspar and Plagioclase feldspar.

show a persistent deficiency of larger cations. They suggested that the deficiency may be explained through deviation from ideal plagioclase stoichiometry towards a higher siliceous solid solution, for example, in pure albite virtue of substitution Si = Na, Al, and in anorthite through Si = Al, 0.5Ca.

Plagioclase contains minor amounts of total iron as FeO. In the feldspar, smaller six co-ordinate divalent cations are not possible on crystal structure ground. Fe is likely present as Fe^{3+} substituting Al^{3+} or possibly due to extremely fine inclusion of opaque in plagioclase which could not be identified under microprobe.

5.9 Sillimanite

The electron microprobe data of the sillimanite and their structural formulae (calculated on the basis of 10 Oxygen) from pelitic granulites is presented in Table 5.9. The composition is relatively pure Al_2SiO_5. The most common ion replacing aluminium in the sillimanite structure is ferric ion while other elements viz. Ti, Cr, Ca, K, Na and Mn are present in minimum amounts. The Al-content ranges between 3.897–3.968 p.f.u. Sillimanite includes minor amounts of Cr and Fe. Total Fe as Fe^{2+} has been analyzed. The Cr and Fe content varies from 0.001 to 0.002 p.f.u and 0.018 to 0.03 p.f.u, respectively.

5.10 Chlorite

Chemical analyses of chlorites were carried out on microprobe, and structural formula (calculated on basis of 14 Oxygen) are given in Table 5.10. The ideal formula of chlorite can be described as; **$[(Mg,Fe)_3(Si,Al)_4O_{10}(OH)_2 \cdot (Mg,Fe)_3(OH)_6]$** (repeating unit).

The analyzed data for chlorite have been plotted in the triangular diagram SiO_2 – (MgO+FeO) – Al_2O_3 (Fig.5.7) for the end-members of chlorite classification (after [315]) for Amesite, Sudoite and Clinochlore-Daphnite in two substitution: - TK: Tschermak substitution; DT: di/tri octahedral substation. Here all data plots close to the Amesite with a few slightly away from Amesite toward the sudoite and thus indicate of Tschermak substitution. Chlorite contains Fe^{2+} and Fe^{3+}, and in some of the chlorite grains, Fe^{3+} exceeds than Fe^{2+}. Also, Al^{IV} and Al^{VI} found in these rocks lie between 0.0 - 0.396 and 1.78 - 5.273 pfu, respectively. BaO is found in trace amount, and X_{Mg} varies from 0.37 to 0.58.

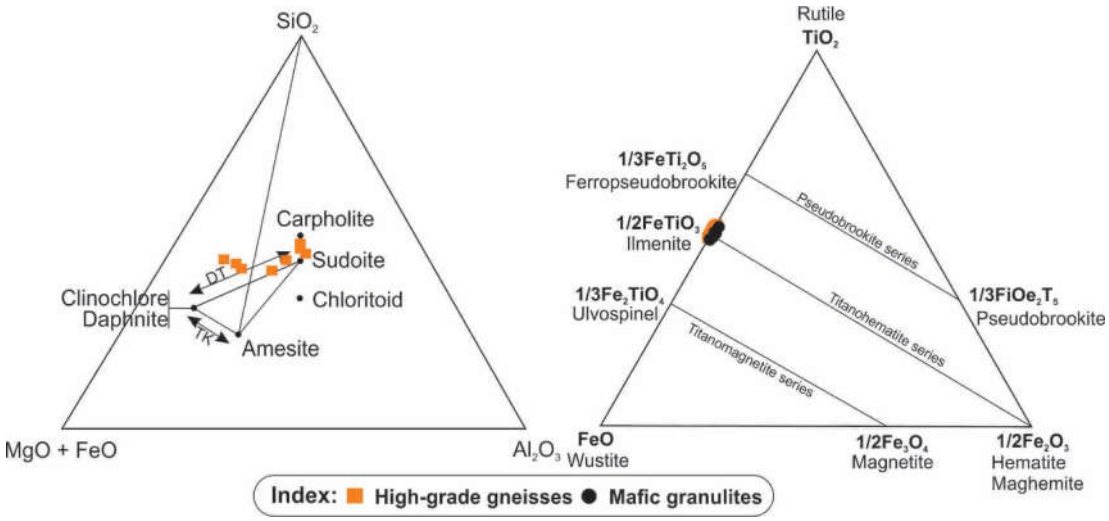

Figure 5.7 Triangular diagram for chlorite end-member; **Fig 5.8** Triangular diagram for ilmenite and magnetite.

5.11 Opaque

These include ilmenite and magnetite. Ilmenite from the gneisses and granulites are presented in Table 5.11. It approximates the ideal formula $(Fe,Mg,Mn)_2Ti_2O_6$. The structural formulae of ilmenite have been calculated on the 6 Oxygen basis. The structural formula deviates slightly from an ideal formula. The total Fe as Fe^{2+} has been analyzed, the deficiency at Ti-site or presence of more than 2 divalent cations suggest the presence of Fe^{3+} in significant amounts. Thus ilmenite calculated on 6 Oxygen was normalized to 4 cations to estimate Fe^{3+} and Fe^{2+} [316] from the formula: $Fe^{3+} = 12 - [2(Fe^{t}+Mn+Mg) + 3(Al+Cr) + 4(Ti)]$.

The calculated structural formulae of ilmenite suggest significant amount of hematite solid solution in ilmenite in most of the samples. Thus this ilmenite may be better termed as hemoilmenite if Fe^{3+} is present significant amounts. Fe^{3+} varies from (0.008 to 0.154 p.f.u). All the analyzed ilmenites have been plotted in the triangular TiO_2–FeO–Fe_2O_3 diagram (Fig.5.8). The plots of ilmenites from gneisses and granulites

lie between TiO_2 and FeO corner. Compositionally, ilmenite of high-grade gneisses are magnesian–mangaon ilmenites (MgO: 0.05–0.73 wt% and MnO: 0.01–0.24 wt%).

5.12 Transmission electron microscopy

Transmission electron microscopy (TEM) analysis was done at the Central Instrumental Facility of the Indian Institute of Technology (BHU) at Varanasi with an FEI-Philips (Type: TECNAI G^1 20 TWIN) operating at 210–240 V.

5.12.1 Gedrite

Gedrite-bearing assemblages have been reported from regionally metamorphosed amphibolite to granulite facies rocks with diverse mineral parageneses from different geological areas [317-321]. The assemblages containing gedrite and hypersthene are more significant in granulite facies rocks because it preserves the textural evidence of gedrite and hypersthene's appearance in the rocks. The occurrence of gedrite-bearing rocks in regional metamorphism from different granulite belts of India has attracted petrologists' attention (The Eastern Ghats, [320]; Southern Granulite, [322]; Rajasthan Granulite, [323]). Cordierite- and gedrite- bearing rocks have attracted considerable attention among petrologists due to their unusual bulk composition and the complex texture, which have preserved during their formation [324]. Their interpretation has wide application for the distribution and behaviour of fluids in metamorphic evolution. The occurrence of multistage gedrite phases, in particular assemblage, serves a better tool to understand the evolution of the rocks during regional metamorphism.

Petrography study also reveals three morphological types of gedrite crystals, which are thoroughly described in Chapter-4. TEM images and selected area electron diffraction (SAED) patterns are analyzed for observation of microstructure of the gedrite.

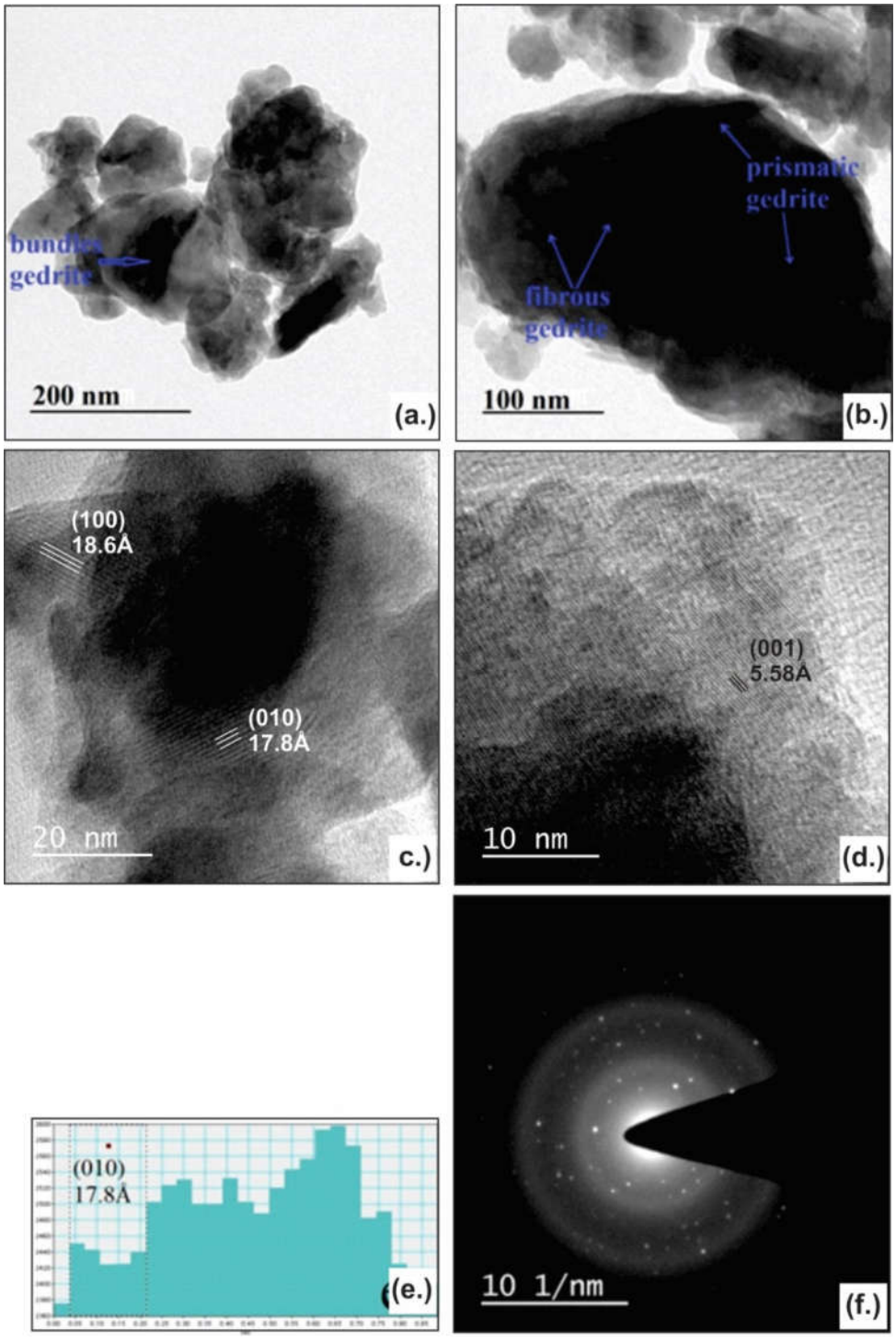

Figure 5.9 TEM images (a) Shows the distribution of gedrite grain in which bundles forms of gedrite grains are present. (b) Fibrous and prismatic growth of gedrite minerals. (c) The orientations of grains are in (100) and (010). (d) The orientation of grain in (001). (e) Width of double-chain silicate structure along (010) orientation with the help of histograph by using TEM. (f) SAED pattern of gedrite grain.

Here, three types i.e., bundles, prismatic and fibrous forms of gedrite have been observed in the TEM image analyses (Fig.5.9a&b). Bundles are assemblages of individual separable particles (they are fibres, but also acicular or prismatic particles, Fig.5.9a). Bundles often show a lack of cohesion between particles in the group; it can be seen by relative displacement among the particles along the bundle's length. Prismatic particles are well-developed crystal faces with low (<10:1) to moderate (10:1 to 20:1) aspect ratios. They have one elongated dimension and two shorter of approximately equal dimensions (i.e., similar particle width and thickness, Fig.5.9b). The sides of prismatic particles are typically parallel. Prismatic particle's edges are well-defined and crystalline. Fibrous forms of gedrite are thin and elongated particles with parallel sides and their surfaces are smooth. Fibres have very high (20:1 to 100:1, or higher) aspect ratios and often display curvature [i.e., bending and flexibility (Fig.5.9b) where the fibre end wraps around another particle]. This classification of amphibole has been given by [325]. TEM image shows the different position occupied by gedrite and arrangement of double-chain silicate structure with all the three axial directions. Unit cell parameter of the gedrite detected by TEM are a-axis=18.6 Å, b-axis = 17.8 Å and c-axis = 5.58 Å (Fig.5.9c-e). It is very similar to gedrite unit cell parameter, i.e., a-axis = 1.8531 nm, b-axis = 1.7741 nm and c-axis = 0.5249 nm; given by [326]. The SAED pattern shows the metallic element position at the different lattice site (Fig.5.9f).

5.12.2 Pyroxene Exsolution

Mineral exsolution is a particular type of texture formed in minerals either by rapid dissociation of fluids from two associated thermodynamic phases or by asymmetric nucleation and crystals development [53, 54, 327]. In metamorphic rocks, development

of exsolution texture is primarily due to reduction in pressure [55-57] and variations in the oxidation state [58], while temperature and oxygen fugacity act as an essential factor in the development of exsolution texture in igneous rocks [59, 60]. Therefore, mineral exsolution textures provide many significant information about the variation in pressure, temperature, oxygen fugacity, and fluid availability during mafic granulites' exhumation.

Most of the clinopyroxenes in the analyzed mafic granulites have shown peculiar exsolution textures of orthopyroxene-rich lamellae (Fig.5.10a&b). The observed orthopyroxene lamellae were very thin, and their composition was difficult to be determined by using EMPA Back Scattered Images (BSE) analysis techniques. Accordingly, Transmission Electron Microscopy (TEM) is used to distinguish the Cpx-Opx minerals and study their mutual intergrowths (Fig.5.10).

TEM investigation has highlighted a contrasting chemical behaviour of opx and cpx at the opx-cpx interface area, with the interface area showing the admixing of the silicate structure of two different minerals i.e, opx and cpx (Fig.5.10d). The measured lattice parameters of Opx and Cpx were: a = 18.4, b = 8.8, c = 5.3 Å and a = 9.4, b = 8.9, c = 5.4 Å respectively determined by electron diffraction pattern [328]. The microstructure of opx and cpx were observed in TEM nanophotographs (Fig.5.10). The microstructure domains were magnified up to 10–20 nm scale, which showed the silicate structure of opx and cpx with different lattice parameters. The selected area electron diffraction (SAED) pattern reflects the ring-like structure, suggesting a crystalline nature for minerals. However, the arrangement of metallic elements was located at different lattice positions (Fig.5.10g). TEM-EDS (Energy-dispersive X-ray spectrometry) analysis revealed the presence of Ca, Mg and Fe contents (Fig.5.10h).

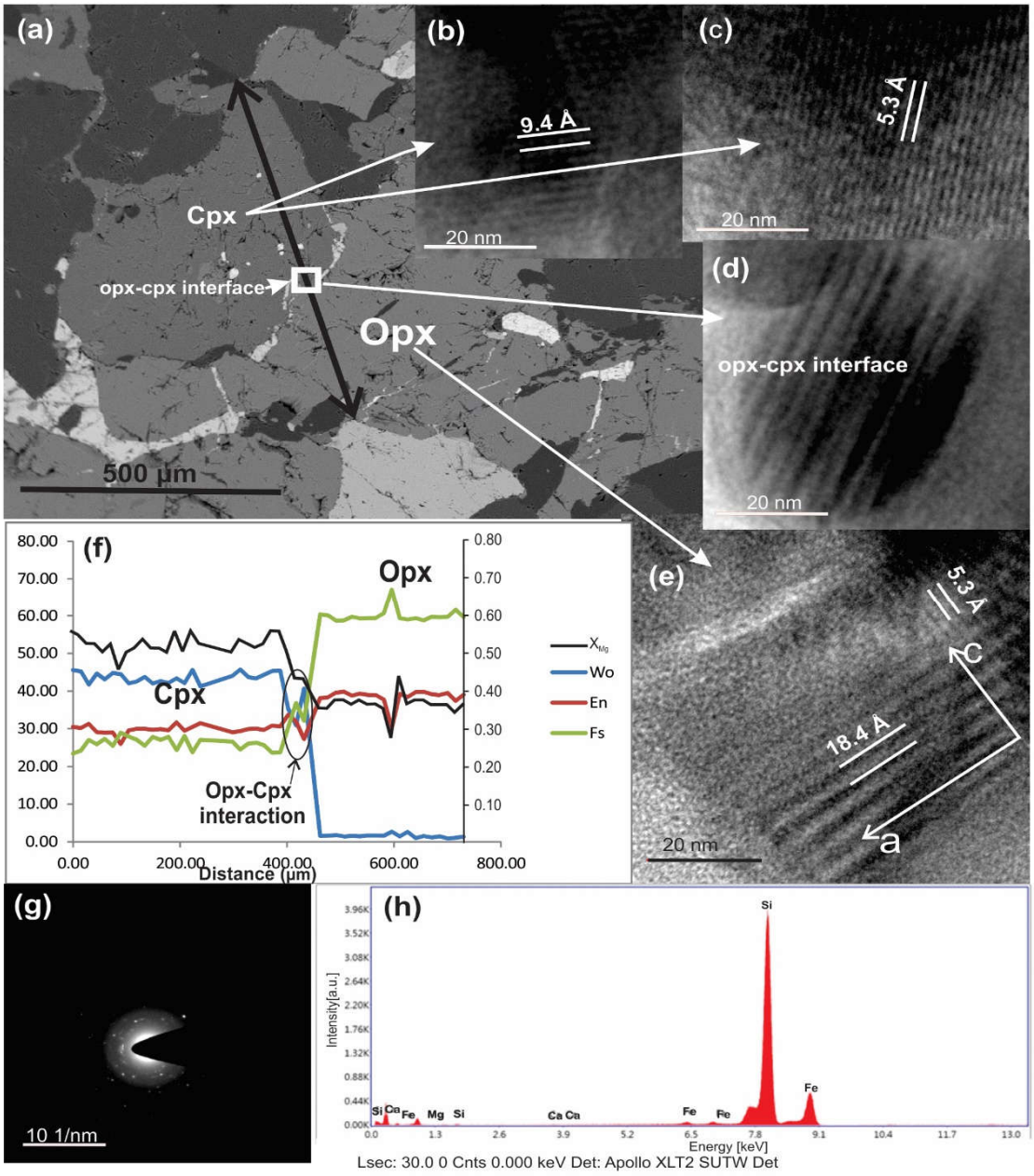

Figure 5.10 (a) Back Scattered Electron (BSE) image shows porphyroblast of Orthopyroxene and Clinopyroxene, with a line along which compositional profiling has been done interface of Opx-Cpx. (b) [100] TEM projection of Cpx. (c) [001] TEM projection of Cpx. (d) Silicate structure of the Opx-Cpx interface. (e) [100] and [001] TEM projection of Opx (f) A line profile along with the Opx-Cpx minerals showing a compositional variation of Wollastonite, Enstatite and Ferrosilite components, with Variation of XMg along with this line profile. (g) SAED pattern of Pyroxene grain. (h) Graphical representation of EDAX values of pyroxene.

Table 5.1 Chemical analysis and structural formulae (on the basis of 12 Oxygen) of garnet from high-grade gneisses.

Sample	R-91-97									
Domain	122 / 142	122 / 143	122/45	122/20	122/ 44	122/46	101	102	103	104
SiO_2	37.45	38.23	37.65	36.56	37.40	37.61	37.89	37.90	37.89	37.76
TiO_2	0.05	bdl	0.005	0.002	0.005	0.011	0.002	0.067	0.017	bdl
Al_2O_3	20.51	20.68	20.19	20.46	20.37	20.37	20.53	20.74	20.84	20.90
FeO	35.14	35.79	34.39	35.82	34.36	34.39	32.02	31.85	32.50	32.38
MnO	0.36	0.38	0.30	0.34	0.48	0.22	0.37	0.26	0.23	0.24
MgO	5.81	5.34	7.28	6.80	7.26	7.10	7.92	7.63	7.99	7.91
CaO	0.27	0.41	0.26	0.24	0.25	0.25	0.28	0.27	0.28	0.27
Total	**99.6**	**100.84**	**100.11**	**100.23**	**100.14**	**99.99**	**99.02**	**98.71**	**99.74**	**99.46**
Si	2.987	3.05	2.963	2.886	2.942	2.965	3.006	3.011	2.986	2.985
Al^{IV}	bdl	bdl	bdl	bdl	bdl	bdl	bdl	bdl	bdl	bdl
ΣZ	2.987	3.05	2.963	2.886	2.942	2.965	3.006	3.011	2.986	2.985
Al^{VI}	1.926	1.91	1.874	1.904	1.889	1.893	1.919	1.941	1.936	1.946
Ti	bdl	bdl	0.001	0.001	0.001	0.001	bdl	0.004	0.001	bdl
Fe^{3+}	0.088	0.032	0.203	0.326	0.229	0.18	0.121	0.056	0.134	0.114
ΣY	2.014	1.942	2.078	2.23	2.119	2.074	2.040	2.001	2.071	2.060
Fe^{2+}	2.259	2.329	2.081	2.039	2.031	2.087	2.021	2.057	2.110	2.080
Mn	0.023	0.033	0.02	0.023	0.032	0.015	0.025	0.017	0.015	0.016
Mg	0.693	0.634	0.864	0.8	0.851	0.834	0.937	0.903	0.939	0.933
Ca	0.024	0.027	0.022	0.02	0.021	0.021	0.024	0.023	0.023	0.023
ΣX	2.999	3.023	2.991	2.884	2.939	2.961	3.007	3.001	3.087	3.052
X_{Mg}	**0.22**	**0.21**	**0.27**	**0.25**	**0.27**	**0.27**	**0.31**	**0.30**	**0.30**	**0.30**
Pyrope	22.3	20.6	28.9	27.8	29.0	28.2	30.1	29.5	30.1	30.0
Almandine	76.1	77.5	69.69	70.7	69.1	70.5	68.3	69.2	68.7	68.8
Grossularite	0.8	1.1	0.74	0.7	0.7	0.7	0.8	0.8	0.8	0.7
Spessartite	0.8	0.8	0.67	0.8	1.2	0.6	0.8	0.6	0.5	0.5

X_{Mg} = Mg/(Fe^{2+}+Mg); bdl = Below Detection Limt

Table 5.1 contd.

	High-grade Gneiss						Pelitic Granulites			
Sample	R-91-96						D-3			
Domain	105	111	68	69	70	123	6	7	10	20
SiO_2	37.23	38.24	38.79	37.82	37.73	37.34	37.85	37.63	38.12	36.83
TiO_2	0.034	0.023	bdl	bdl	bdl	0.012	0.022	0.113	0.044	0.055
Al_2O_3	20.97	19.38	20.48	20.49	20.62	20.30	20.89	20.85	20.92	21.08
FeO	32.70	35.26	31.72	31.66	31.58	34.67	36.42	36.33	35.29	34.78
MnO	0.38	0.42	0.25	0.36	0.23	0.21	0.62	0.58	0.57	0.63
MgO	7.76	5.48	7.76	8.13	7.89	6.64	4.29	4.47	5.28	5.09
CaO	0.28	0.36	0.35	0.5	0.58	0.26	0.69	0.63	0.61	0.72
Total	**99.35**	**99.18**	**99.36**	**98.986**	**98.64**	**99.43**	**100.76**	**100.59**	**100.83**	**99.18**
Si	2.956	3.076	3.054	2.997	2.998	2.989	3.010	2.998	3.013	2.966
Al^{IV}	bdl	bdl	bdl	bdl	bdl	bdl	bdl	bdl	bdl	bdl
ΣZ	2.956	3.076	3.054	2.997	2.998	2.989	3.010	2.998	3.013	2.966
Al^{VI}	1.963	1.837	1.9	1.914	1.930	1.914	1.958	1.958	1.949	2.001
Ti	0.002	0.001	bdl	bdl	bdl	0.001	0.001	0.007	0.003	0.003
Fe^{3+}	0.125	0.011	bdl	0.006	0.018	0.104	0.006	0.006	0.000	0.001
ΣY	2.090	1.85	1.889	1.920	1.948	2.018	1.966	1.971	1.951	2.005
Fe^{2+}	2.056	2.361	2.097	2.098	2.098	2.214	2.422	2.420	2.333	2.342
Mn	0.026	0.029	0.017	0.024	0.016	0.014	0.041	0.039	0.038	0.043
Mg	0.919	0.657	0.911	0.960	0.935	0.792	0.508	0.531	0.622	0.611
Ca	0.023	0.031	0.03	0.043	0.049	0.023	0.058	0.054	0.052	0.062
ΣX	3.024	3.077	3.054	3.126	3.098	3.043	3.030	3.044	3.045	3.058
X_{Mg}	**0.30**	**0.21**	**0.30**	**0.31**	**0.31**	**0.25**	**0.17**	**0.18**	**0.21**	**0.21**
Pyrope	29.7	21.3	29.9	30.7	30.9	25.1	16.8	17.4	20.4	12.0
Almandine	69.8	76.8	68.5	67.1	67.7	73.7	79.9	79.5	76.6	76.6
Grossularite	0.7	1	1	1.4	1.6	0.7	1.9	1.8	1.7	2.0
Spessartite	0.8	0.9	0.6	0.8	0.5	0.5	1.4	1.3	1.3	1.4

X_{Mg} = Mg/(Fe^{2+}+Mg); bdl = Below Detection Limt

Table 5.1 contd.

	Pelitic Granulite					Mafic Granulites				
Sample	D-3					RP-5				
Domain	8	9	11	12	13	6	7	9	12	14
SiO_2	37.64	37.57	37.46	38.02	38.15	37.16	36.79	36.76	37.23	36.85
TiO_2	0.024	0.062	0.059	bdl	0.025	0.042	0.021	0.044	0.053	0.034
Al_2O_3	20.85	21.38	21.18	20.96	21.02	21.23	21.24	21.23	21.25	21.42
FeO	34.08	34.82	34.99	33.79	34.39	20.38	20.51	20.08	20.12	20.12
MnO	0.52	0.43	0.68	0.47	0.59	11.38	11.77	12.12	11.75	11.67
MgO	5.45	5.74	5.88	5.54	5.31	3.71	3.57	3.59	3.53	3.49
CaO	1.09	0.62	0.66	0.90	0.83	6.62	6.77	6.94	6.73	6.78
Total	**99.65**	**100.61**	**100.91**	**99.67**	**100.32**	**100.52**	**100.67**	**100.76**	**100.66**	**100.37**
Si	3.003	2.971	2.962	3.022	3.020	2.948	2.926	2.922	2.951	2.932
Al^{IV}	bdl	bdl	bdl	bdl	bdl	0.014	0.020	0.010	0.008	0.014
ΣZ	3.003	2.971	2.962	3.022	3.020	2.962	2.946	2.932	2.959	2.946
Al^{VI}	1.960	1.993	1.973	1.963	1.961	1.985	1.990	1.988	1.985	2.009
Ti	0.001	0.004	0.004	bdl	0.002	0.003	0.001	0.003	0.003	0.002
Fe^{3+}	0.001	0.000	0.002	0.000	0.000	0.003	0.002	0.002	0.002	0.003
ΣY	1.963	1.996	1.979	1.964	1.963	1.990	1.994	1.993	1.990	2.013
Fe^{2+}	2.273	2.303	2.313	2.246	2.277	1.351	1.364	1.335	1.334	1.338
Mn	0.035	0.029	0.046	0.032	0.039	0.765	0.793	0.816	0.789	0.786
Mg	0.648	0.677	0.693	0.656	0.627	0.439	0.424	0.425	0.417	0.413
Ca	0.093	0.053	0.056	0.077	0.071	0.562	0.577	0.591	0.571	0.578
ΣX	3.049	3.061	3.107	3.011	3.014	3.117	3.158	3.166	3.111	3.116
X_{Mg}	**0.22**	**0.23**	**0.23**	**0.23**	**0.22**	**0.25**	**0.24**	**0.24**	**0.24**	**0.24**
Pyrope	21.2	22.1	22.3	21.8	20.8	14.1	13.4	13.4	13.4	13.3
Almandine	74.6	75.2	74.5	74.6	75.5	43.4	43.2	42.6	42.9	43.0
Grossularite	3.1	1.7	1.8	2.6	2.3	18.0	18.3	18.7	18.4	18.6
Spessartite	1.1	0.9	1.5	1.1	1.3	24.5	25.1	25.8	25.4	25.2

X_{Mg} = $Mg/(Fe^{2+}+Mg)$; bdl = Below Detection Limt

Table 5.2 Chemical analysis and structural formulae (on the basis of 23 Oxygen) of Hornblende from mafic granulite.

Sample No.	RP-1									
Domain	121	122	123	124	125	126	127	128	129	130
SiO_2	40.49	40.44	41.83	41.89	40.23	41.81	41.85	41.87	41.65	41.98
TiO_2	1.72	2.38	2.25	1.86	1.98	2.28	1.99	2.25	2.35	2.26
Al_2O_3	11.38	11.99	10.53	9.86	13.11	10.46	10.53	11.06	10.67	9.85
Cr_2O_3	0.25	0.28	0.7	0.1	0.26	0.17	0.21	0.21	0.24	0.08
FeO	20.53	19.99	20.01	20.62	19.81	20.87	21.48	19.83	20.92	21.65
MnO	0.12	0.15	0.08	0.29	0.24	0.18	0.02	0.26	0.13	0.23
MgO	7.7	7.16	7.73	7.86	7.14	7.33	7.75	8.16	7.99	7.73
NiO	0.15	0.01	0.15	0.01	0.12	0.08	0.09	0.17	0.26	bdl
CaO	11.23	11.36	11.37	10.66	10.57	10.85	11.18	11.5	11.34	11.29
Na_2O	1.07	1.17	1.12	1.18	0.99	1.15	1.22	1.12	1	0.94
K_2O	1.68	1.79	1.71	1.59	1.56	1.43	1.48	1.38	1.44	1.41
F	0.23	0.29	0.36	0.17	0.11	0.22	0.24	0.1	0.25	0.33
Cl	0.1	0.14	0.09	0.15	0.12	0.14	0.09	0.09	0.06	0.09
Total	**96.65**	**97.15**	**97.93**	**96.24**	**96.24**	**96.97**	**98.13**	**98.0**	**98.3**	**97.84**
Si	6.195	6.145	6.378	6.481	6.125	6.456	6.429	6.304	6.335	6.487
Al^{iv}	1.805	1.855	1.622	1.519	1.875	1.544	1.571	1.696	1.665	1.513
ΣZ	8	8	8	8	8	8	8	8	8	8
Al^{vi}	0.291	0.372	0.352	0.171	0.478	0.359	0.335	0.266	0.247	0.281
Ti	0.2	0.276	0.258	0.216	0.227	0.265	0.230	0.255	0.269	0.263
Cr	0.031	0.034	0.084	0.012	0.031	0.021	0.026	0.025	0.029	0.010
Fe^{+3}	0.619	0.342	0.372	0.592	0.868	0.418	0.417	0.593	0.581	0.400
Fe^{+2}	2.016	2.285	2.229	2.048	1.730	2.216	2.204	1.976	2.014	2.237
Mn	0.016	0.02	0.01	0.038	0.031	0.024	0.003	0.033	0.017	0.030
Mg	1.773	1.643	1.757	1.813	1.621	1.687	1.775	1.831	1.812	1.781
Ni	0.019	0.001	0.018	0.001	0.015	0.010	0.011	0.021	0.032	bdl
ΣX	5.001	5.001	4.998	4.999	5.000	5.000	5.000	5.000	5.000	5.000
Ca	1.859	1.874	1.857	1.767	1.724	1.795	1.840	1.855	1.848	1.869
Na	0.32	0.349	0.331	0.354	0.292	0.344	0.363	0.327	0.295	0.282
K	0.331	0.352	0.333	0.314	0.303	0.282	0.290	0.265	0.279	0.278
ΣY	2.51	2.575	2.521	2.435	2.320	2.421	2.493	2.447	2.422	2.429
F	0.112	0.141	0.174	0.083	0.053	0.107	0.117	0.048	0.120	0.161
Cl	0.026	0.037	0.023	0.039	0.031	0.037	0.023	0.023	0.015	0.024
X_{Mg}	**0.40**	**0.38**	**0.40**	**0.41**	**0.38**	**0.39**	**0.40**	**0.42**	**0.41**	**0.40**

X_{Mg} = Mg/(Fe^{2+}+Mg); bdl = Below Detection Limt

Table 5.2 contd.

Sample	D-8									
Domain	41	42	43	44	45	46	47	48	49	50
SiO_2	42.63	43.02	42.28	42.27	42.39	42.87	41.86	42.49	42.58	42.39
TiO_2	2.21	1.77	2.31	2.13	2.21	2.06	2.12	2.08	2.13	2.2
Al_2O_3	10.01	10.61	10.59	10.57	10.39	10.19	10.48	10.28	10.41	10.24
Cr_2O_3	0.06	0.01	0.25	0.11	0.03	0.08	0.13	0.11	0.12	0.03
FeO	19.25	19.22	18.72	18.27	18.88	17.99	18.96	18.57	18.44	19.64
MnO	0.31	0.19	0.17	0.24	0.15	0.09	0.28	0.3	0.23	0.26
MgO	8.99	8.89	8.66	8.98	8.63	9.09	8.87	8.95	8.62	8.98
NiO	bdl	0.1	0.11	bdl	0.08	0.04	Bdl	0.11	bdl	0.03
CaO	11.61	11.38	11.13	11.25	11.29	11.38	11.12	11.42	11.29	11.27
Na_2O	1.18	1.2	1.38	1.4	1.39	1.43	1.38	1.37	1.34	1.3
K_2O	1.51	1.46	1.49	1.4	1.49	1.39	1.43	1.41	1.36	1.35
F	0.36	0.25	0.3	0.35	0.39	0.25	0.24	0.28	0.33	0.17
Cl	0.17	0.19	0.18	0.18	0.16	0.16	0.15	0.17	0.19	0.16
Total	**98.29**	**98.29**	**97.57**	**97.15**	**97.48**	**97.02**	**97.02**	**97.54**	**97.04**	**98.02**
Si	6.380	6.397	6.325	6.311	6.375	6.390	6.296	6.349	6.388	6.347
Al^{iv}	1.620	1.603	1.675	1.689	1.625	1.610	1.704	1.651	1.612	1.653
ΣZ	8.000	8.000	8.000	8.000	8.000	8.000	8.000	8.000	8.000	8.000
Al^{vi}	0.146	0.257	0.192	0.171	0.217	0.180	0.154	0.159	0.229	0.154
Ti	0.249	0.198	0.260	0.239	0.250	0.231	0.240	0.234	0.240	0.248
Cr	0.007	0.001	0.030	0.013	0.004	0.009	0.015	0.013	0.014	0.004
Fe^{+3}	0.615	0.699	0.681	0.755	0.575	0.645	0.794	0.689	0.609	0.750
Fe^{+2}	1.938	1.838	1.871	1.793	1.991	1.898	1.772	1.860	1.951	1.804
Mn	0.039	0.024	0.022	0.030	0.019	0.011	0.036	0.038	0.029	0.033
Mg	2.006	1.971	1.931	1.999	1.935	2.020	1.989	1.994	1.928	2.004
Ni	bdl	0.012	0.013	bdl	0.010	0.005	Bdl	0.013	bdl	0.004
ΣX	5.000	5.000	5.000	5.000	5.000	5.000	5.000	5.000	5.000	5.000
Ca	1.862	1.813	1.784	1.800	1.819	1.817	1.792	1.828	1.815	1.808
Na	0.342	0.346	0.400	0.405	0.405	0.413	0.402	0.397	0.390	0.377
K	0.288	0.277	0.284	0.267	0.286	0.264	0.274	0.269	0.260	0.258
ΣY	2.492	2.436	2.469	2.472	2.510	2.495	2.469	2.494	2.465	2.443
F	0.170	0.118	0.142	0.165	0.186	0.118	0.114	0.132	0.157	0.080
Cl	0.043	0.048	0.046	0.046	0.041	0.040	0.038	0.043	0.048	0.041
$\mathbf{X_{Mg}}$	**0.44**	**0.44**	**0.43**	**0.44**	**0.43**	**0.44**	**0.44**	**0.44**	**0.43**	**0.44**

X_{Mg} = Mg/(Fe^{2+}+Mg); bdl = Below Detection Limt

Table 5.2 contd.

Sample	K-1										
Domain	14	15	27	28	36	42	43	44	45	46	47
SiO_2	45.32	45.02	45.08	44.65	45.12	44.71	44.73	44.14	44.36	43.69	44.13
TiO_2	1.56	1.67	1.37	1.46	1.78	1.67	1.77	1.67	1.83	1.56	1.73
Al_2O_3	8.75	8.89	9.27	8.54	9.17	8.98	9.28	9.16	9.39	9.38	9.26
Cr_2O_3	0.07	0.07	0.34	0.08	0.21	0.05	0.09	0.32	0.23	0.10	0.27
FeO	14.92	15.38	15.74	16.84	15.42	15.54	16.54	15.21	15.57	16.21	16.17
MnO	0.17	0.14	0.15	0.14	0.21	0.14	0.14	0.22	0.23	0.17	0.24
MgO	11.98	11.68	11.96	11.37	11.47	12.27	11.69	12.37	11.77	11.67	11.88
NiO	0.08	0.11	bdl	0.07	0.05	0.09	0.07	0.18	bdl	0.05	0.09
CaO	11.62	11.27	11.34	10.96	11.54	11.26	11.72	11.84	11.29	11.85	11.79
Na_2O	0.95	0.98	0.96	0.99	0.98	1.10	0.99	0.96	1.03	0.99	0.99
K_2O	0.89	0.99	1.00	0.87	0.94	1.02	1.01	0.88	0.93	0.97	0.98
F	0.06	0.16	0.08	0.23	0.08	bdl	0.01	0.22	0.04	0.20	0.13
Cl	0.09	0.08	0.07	0.05	0.07	0.11	0.09	0.09	0.07	0.07	0.10
Total	**96.46**	**96.44**	**97.36**	**96.25**	**97.04**	**96.94**	**98.13**	**97.26**	**96.74**	**96.91**	**97.76**
Si	6.405	6.397	6.348	6.445	6.389	6.309	6.339	6.218	6.283	6.266	6.263
Al^{iv}	1.457	1.489	1.538	1.453	1.530	1.493	1.550	1.521	1.567	1.586	1.549
ΣZ	7.862	7.886	7.886	7.898	7.919	7.802	7.889	7.739	7.850	7.852	7.811
Al^{vi}	bdl	bdl	bdl	bdl	bdl	bdl	bdl	bdl	bdl	bdl	bdl
Ti	0.166	0.178	0.145	0.159	0.190	0.177	0.189	0.177	0.195	0.168	0.185
Cr	0.008	0.008	0.038	0.009	0.024	0.006	0.010	0.036	0.026	0.011	0.030
Fe^{+3}	1.454	1.471	1.574	1.504	1.349	1.640	1.371	1.658	1.574	1.439	1.491
Fe^{+2}	0.957	0.953	0.828	0.959	1.067	0.767	1.047	0.745	0.842	1.008	0.930
Mn	0.020	0.017	0.018	0.017	0.025	0.017	0.017	0.026	0.028	0.021	0.029
Mg	2.524	2.474	2.511	2.447	2.421	2.581	2.470	2.598	2.485	2.495	2.513
Ni	0.009	0.013	bdl	0.008	0.006	0.010	0.008	0.020	bdl	0.006	0.010
ΣX	5.138	5.114	5.114	5.102	5.081	5.198	5.111	5.261	5.150	5.148	5.189
Ca	1.759	1.716	1.711	1.695	1.751	1.702	1.780	1.787	1.713	1.821	1.793
Na	0.260	0.270	0.262	0.277	0.269	0.301	0.272	0.262	0.283	0.275	0.272
K	0.160	0.179	0.180	0.160	0.170	0.184	0.183	0.158	0.168	0.177	0.177
ΣY	2.180	2.165	2.153	2.132	2.190	2.187	2.234	2.208	2.164	2.274	2.242
F	0.027	0.072	0.036	0.105	0.036	bdl	0.004	0.098	0.018	0.091	0.058
Cl	0.022	0.019	0.017	0.012	0.017	0.026	0.022	0.021	0.017	0.017	0.024
X_{Mg}	**0.51**	**0.51**	**0.51**	**0.50**	**0.50**	**0.52**	**0.51**	**0.52**	**0.51**	**0.50**	**0.51**

X_{Mg} = Mg/(Fe^{2+}+Mg); bdl = Below Detection Limt

Table 5.3 Chemical analysis and structural formulae (on the basis of 23 Oxygen) of Gedrite from high-grade gneisses.

Sample	R-91-97							R-91-96			
Domain	133	134	171	174	176	175	176	11	12	86	87
SiO_2	44.49	45.15	44.7	49.81	44.91	44.43	44.91	46.85	48.75	45.68	46.39
TiO_2	0.22	0.22	0.39	0.02	0.26	0.32	0.26	bdl	bdl	0.22	bdl
Al_2O_3	12.3	11.36	11.65	6.39	11.83	12.01	11.83	10.97	10.34	11.52	10.24
FeO	21.59	22.41	22.39	22.04	22.53	21.81	22.53	21.01	20.49	21.72	21.41
MgO	15.51	15.57	14.9	16.99	14.98	14.73	14.98	16	17.16	15.57	16.19
CaO	0.09	0.1	0.13	0.08	0.10	0.11	0.09	0.03	0.05	0.05	0.08
Na_2O	1.5	1.47	1.6	0.79	1.61	1.67	1.61	1.82	1.12	1.61	1.31
BaO	0.24	0.37	0.2	0.31	0.34	0.41	0.34	bdl	bdl	0.20	0.24
F	0.4	0.43	0.34	0.28	0.22	0.46	0.22	0.36	0.19	0.34	0.37
Total	**96.49**	**97.14**	**96.33**	**96.76**	**96.88**	**96.08**	**96.88**	**97.04**	**98.09**	**96.94**	**96.23**
Si	6.65	6.72	6.71	7.36	6.704	6.69	6.7	6.893	7.024	6.772	6.912
Al^{iv}	1.35	1.28	1.29	0.64	1.296	1.31	1.3	1.107	0.976	1.228	1.088
ΣZ	8	8	8	8	8	8	8	8	8	8	8
Al^{vi}	0.81	0.71	0.77	0.472	0.785	0.83	0.78	0.796	0.78	0.786	0.71
Ti	0.02	0.02	0.04	0.002	0.029	0.04	0.03	bdl	bdl	0.025	bdl
Fe^{3+}	0.03	0.05	bdl	bdl	bdl	bdl	bdl	bdl	bdl	bdl	bdl
Fe^{2+}	2.66	2.74	2.81	2.723	2.812	2.75	2.81	2.585	2.469	2.693	2.667
Mg	3.45	3.46	3.33	3.741	3.333	3.31	3.33	3.51	3.686	3.441	3.596
ΣX	6.99	6.98	6.95	6.938	6.959	6.92	6.96	6.095	6.155	6.945	6.974
Ca	0.01	0.02	0.02	0.013	0.015	0.02	0.02	0.004	0.007	0.008	0.012
Na	0.43	0.42	0.47	0.227	0.467	0.49	0.47	0.519	0.313	0.463	0.378
Ba	0.01	0.02	0.01	0.017	0.02	0.02	0.02	bdl	bdl	0.012	0.014
Σy	0.46	0.46	0.5	0.258	0.502	0.53	0.5	0.523	0.32	0.483	0.403
F	0.19	0.2	0.16	0.128	0.105	0.22	0.11	0.169	0.086	0.16	0.174
OH*	1.81	1.8	1.84	1.872	1.895	1.78	1.89	1.831	1.914	1.84	1.826
X_{Mg}	**0.56**	**0.55**	**0.54**	**0.58**	**0.54**	**0.55**	**0.54**	**0.58**	**0.60**	**0.56**	**0.57**

X_{Mg} = $Mg/(Fe^{2+}+Mg)$; bdl = Below Detection Limt

Table 5.4 Chemical analysis and structural formulae (on the basis of 6 Oxygen) of Orthopyroxene from high-grade gneisses.

Sample	R-91-97									
Domain	71	73	75	76	79	80	155	146	74	72
SiO_2	49.14	48.79	48.93	49.07	48.63	48.27	52.13	52.87	49.88	49.86
TiO_2	bdl	bdl	bdl	bdl	bdl	bdl	Bdl	bdl	bdl	bdl
Al_2O_3	2.89	2.91	2.97	2.73	3.13	3.42	3.80	3.29	2.67	2.81
FeO	28.78	28.45	28.71	30.32	28.54	28.90	23.98	23.17	28.82	28.68
MnO	bdl	bdl	bdl	bdl	bdl	bdl	Bdl	bdl	bdl	bdl
MgO	17.93	17.97	17.54	17.75	17.94	17.32	18.33	18.16	17.86	17.87
CaO	0.02	0.05	0.03	bdl	0.025	0.04	0.05	0.05	0.04	0.03
Na_2O	bdl	0.01	0.01	0.02	0.06	0.007	0.57	0.49	bdl	0.07
Total	**98.77**	**98.18**	**98.19**	**99.89**	**98.33**	**98.15**	**98.85**	**98.37**	**99.26**	**99.31**
Si	1.912	1.909	1.915	1.902	1.901	1.898	1.968	2.001	1.928	1.925
Ti	bdl	bdl	bdl	bdl	bdl	bdl	Bdl	bdl	bdl	bdl
Al	0.132	0.134	0.137	0.124	0.144	0.159	0.169	0.147	0.121	0.128
Fe^{3+}	0.065	0.074	0.051	0.109	0.087	0.070	0.000	0.000	0.035	0.041
Fe^{2+}	0.866	0.851	0.885	0.865	0.839	0.875	0.763	0.744	0.894	0.882
Mn	bdl	bdl	bdl	bdl	bdl	bdl	Bdl	bdl	bdl	bdl
Mg	1.040	1.048	1.023	1.026	1.045	1.015	1.031	1.025	1.029	1.029
Ca	0.001	0.002	0.001	bdl	0.001	0.002	0.002	0.002	0.002	0.001
Na	bdl	0.001	0.001	0.002	0.005	0.001	0.042	0.036	bdl	0.005
Total	4.017	4.019	4.013	4.028	4.022	4.018	3.975	3.954	4.009	4.011
End member										
X_{Wo}	0.1	0.1	0.1	0.0	0.1	0.1	0.1	0.1	0.1	0.1
X_{En}	52.7	53.1	52.2	51.3	52.9	51.7	56.1	56.7	52.5	52.6
X_{Fs}	47.2	46.8	47.7	48.7	47.0	48.2	43.5	43.2	47.4	47.3
X_{Mg}	**0.53**	**0.53**	**0.52**	**0.51**	**0.53**	**0.52**	**0.57**	**0.58**	**0.54**	**0.54**

$X_{Wo} = Ca/(Ca+Mg+Fe^T)$; $X_{En} = Mg/(Ca+Mg+Fe^T)$; $X_{Fs} = Fe^T/(Ca+Mg+Fe^T)$; $X_{Mg} = Mg/(Fe^{2+}+Mg)$; bdl = Below Detection Limt

Table 5.4. contd. (from mafic granulites**)**

Sample	RP-1							D-8		
Domain	90	97	83	84	85	86	88	90	8	9
SiO_2	49.81	49.09	49.41	49.71	49.85	50.1	49.95	50.34	51.35	50.87
TiO_2	0.12	0.08	0.11	0.1	0.12	0.13	0.14	0.15	0.08	0.13
Al_2O_3	0.4	0.44	0.45	0.38	0.36	0.31	0.79	0.61	0.71	0.68
Cr_2O_3	0.07	0.07	0.11	0.07	0.07	0.06	0.03	0.03	0.03	bdl
FeO	34.07	35.82	35.23	35.45	35.36	34.16	31.58	30.97	30.62	30.26
MnO	0.93	0.97	0.77	0.91	0.87	0.72	1.12	1.15	1.13	0.89
MgO	13.01	13.45	12.62	13.15	12.99	13.17	15.28	15.75	15.36	15.89
CaO	1.04	0.7	0.87	0.75	0.73	0.81	0.94	0.69	0.76	0.71
Na_2O	bdl	bdl	bdl	bdl	bdl	bdl	0.03	0.03	0.01	0.01
Total	**99.51**	**100.67**	**99.59**	**100.54**	**100.38**	**99.52**	**99.86**	**99.72**	**100.05**	**99.44**
Si	1.99	1.94	1.977	1.967	1.977	1.998	1.95	1.97	2.003	1.989
Ti	bdl	bdl	0.003	0.003	0.004	0.004	Bdl	bdl	0.002	0.004
Al	0.02	0.02	0.021	0.018	0.017	0.015	0.04	0.03	0.033	0.031
Cr	bdl	bdl	0.003	0.002	0.002	0.002	Bdl	bdl	0.001	bdl
Fe^{+3}	bdl	0.1	0.015	0.041	0.02	bdl	0.05	0.03	bdl	bdl
Fe^{+2}	1.14	1.09	1.164	1.132	1.152	1.139	0.99	0.98	0.999	0.99
Mn	0.03	0.03	0.026	0.03	0.029	0.024	0.04	0.04	0.037	0.029
Mg	0.77	0.79	0.753	0.776	0.768	0.783	0.89	0.92	0.893	0.926
Ca	0.04	0.03	0.037	0.032	0.031	0.035	0.04	0.03	0.032	0.03
Na	bdl	bdl	bdl	bdl	bdl	bdl	Bdl	bdl	0.001	0.001
Total	4	4	4	4	4	4	4	4	4	4
End member										
X_{Wo}	2.3	1.5	1.9	1.6	1.6	1.8	2.0	1.5	1.7	1.5
X_{En}	39.6	39.5	38.2	39.2	39.0	40.0	45.4	46.9	46.4	47.6
X_{Fs}	58.2	59.0	59.9	59.2	59.5	58.2	52.6	51.7	51.9	50.9
X_{Mg}	**0.41**	**0.40**	**0.39**	**0.40**	**0.40**	**0.41**	**0.46**	**0.48**	**0.47**	**0.48**

$X_{Wo} = Ca/(Ca+Mg+Fe^T)$; $X_{En} = Mg/(Ca+Mg+Fe^T)$; $X_{Fs} = Fe^T/(Ca+Mg+Fe^T)$; $X_{Mg} = Mg/(Fe^{2+}+Mg)$; bdl = Below Detection Limt

Table 5.4 contd. (from mafic granulites**)**

Sample No.	K-2					D-8				
Domain	24	25	26	17	18	10	11	12	13	14
SiO_2	51.13	50.96	51.61	51.32	51.58	51.13	50.95	51.19	51.07	51.29
TiO_2	0.09	0.02	0.02	0.05	0.17	0.09	0.07	0.06	0.06	0.11
Al_2O_3	0.56	0.44	0.28	0.39	0.47	0.56	0.64	0.48	0.51	0.52
Cr_2O_3	0.02	0.1	0.07	0.09	0.1	0.02	0.03	0.02	0.02	0.03
FeO	31.34	27.93	28.46	28.19	27.91	31.34	30.88	30.19	31.50	30.66
MnO	0.88	0.62	0.61	0.87	0.88	0.88	1.12	1.07	1.18	1.17
MgO	15.22	18.29	18.77	18.13	17.68	15.22	15.17	15.21	15.32	15.50
CaO	0.79	0.59	0.6	0.47	0.63	0.79	0.62	1.82	0.68	0.68
Na_2O	0.02	bdl	bdl	bdl	bdl	bdl	Bdl	bdl	bdl	bdl
Total	**100.05**	**99.01**	**100.42**	**99.55**	**99.42**	**100.05**	**99.49**	**100.06**	**100.34**	**99.99**
Si	1.997	1.97	1.97	1.979	1.994	1.997	2.001	1.995	1.990	2.001
Ti	0.003	bdl	bdl	0.001	0.005	0.003	0.002	0.002	0.002	0.003
Al	0.026	0.02	0.01	0.018	0.021	0.026	0.030	0.022	0.023	0.024
Cr	0.001	bdl	bdl	0.003	0.003	0.001	0.001	0.001	0.001	0.001
Fe^{+3}	bdl	0.03	0.05	0.019	bdl	bdl	Bdl	bdl	bdl	bdl
Fe^{+2}	1.024	0.87	0.86	0.89	0.902	1.024	1.014	0.984	1.027	1.000
Mn	0.029	0.02	0.02	0.028	0.029	0.029	0.037	0.035	0.039	0.039
Mg	0.886	1.05	1.07	1.042	1.019	0.886	0.888	0.884	0.890	0.901
Ca	0.033	0.02	0.02	0.019	0.026	0.033	0.026	0.076	0.028	0.028
Na	0.002	bdl	bdl	bdl	bdl	0.002	0.001	0.002	bdl	0.002
Total	4	4	4	4	4	4	4	4	4	4
End member										
X_{Wo}	1.7	1.2	1.2	1.0	1.3	1.7	1.4	3.9	1.5	1.5
X_{En}	45.6	53.2	53.4	52.9	52.3	45.6	46.0	45.5	45.8	46.7
X_{Fs}	52.7	45.6	45.4	46.1	46.4	52.7	52.6	50.6	52.8	51.8
X_{Mg}	**0.46**	**0.54**	**0.54**	**0.53**	**0.53**	**0.46**	**0.47**	**0.47**	**0.46**	**0.47**

$X_{Wo} = Ca/(Ca+Mg+Fe^T)$; $X_{En} = Mg/(Ca+Mg+Fe^T)$; $X_{Fs} = Fe^T/(Ca+Mg+Fe^T)$; $X_{Mg} = Mg/(Fe^{2+}+Mg)$; bdl = Below Detection Limt

Table 5.5 Chemical analysis and structural formulae (on the basis of 6 Oxygen) of Clinopyroxene from mafic granulites.

Sample No.	RP-1									
Domain	81	82	92	93	93	94	95	96	98	100
SiO_2	50.95	50.93	50.58	50.75	50.75	50.97	51.48	50.97	51.01	51.22
TiO_2	0.08	0.14	0.19	0.12	0.12	0.15	0.17	0.15	0.18	0.15
Al_2O_3	1.05	0.9	0.84	0.86	0.86	0.98	0.92	0.99	0.78	0.55
Cr_2O_3	0.03	0.07	0.05	0.04	0.04	0.09	0.07	0.06	0.07	0.02
FeO	14.96	16.28	16.53	15.89	15.89	15.13	15.68	14.93	17.05	24.54
MnO	0.32	0.47	0.39	0.44	0.44	0.43	0.54	0.44	0.35	0.68
MgO	9.95	9.97	10.52	10.25	10.25	9.98	9.96	9.98	10.14	11.44
CaO	21.98	20.32	20.28	21.55	21.55	21.31	20.43	21.56	20.09	11.76
Na_2O	0.17	0.1	0.12	0.11	0.11	0.19	0.11	0.12	0.18	bdl
Total	**99.52**	**99.2**	**99.5**	**100.01**	**100.01**	**99.26**	**99.37**	**99.2**	**99.85**	**100.38**
Si	1.964	1.978	1.954	1.949	1.949	1.972	1.994	1.970	1.970	1.994
Ti	0.002	0.004	0.006	0.003	0.003	0.004	0.005	0.004	0.008	0.004
Al	0.048	0.041	0.038	0.039	0.039	0.045	0.042	0.050	0.040	0.025
Cr	0.001	0.002	0.002	0.001	0.001	0.003	0.002	0.000	0.000	0.001
Fe^{+3}	0.031	bdl	0.051	0.062	0.062	0.015	bdl	0.010	0.030	bdl
Fe^{+2}	0.451	0.529	0.483	0.448	0.448	0.475	0.508	0.470	0.520	0.799
Mn	0.010	0.015	0.013	0.014	0.014	0.014	0.018	0.010	0.010	0.022
Mg	0.572	0.577	0.606	0.587	0.587	0.576	0.575	0.580	0.580	0.664
Ca	0.908	0.846	0.839	0.887	0.887	0.883	0.848	0.890	0.830	0.491
Na	0.013	0.008	0.009	0.008	0.008	0.014	0.008	0.010	0.010	bdl
Total	4	4	4	4	4	4	4	4	4	4
End member										
X_{Wo}	46.3	43.3	42.4	44.7	44.7	45.3	43.9	45.8	42.3	25.1
X_{En}	29.2	29.6	30.6	29.6	29.6	29.5	29.8	29.5	29.7	34.0
X_{Fs}	24.6	27.1	27.0	25.7	25.7	25.2	26.3	24.7	28.0	40.9
X_{Mg}	**0.54**	**0.52**	**0.53**	**0.53**	**0.54**	**0.54**	**0.53**	**0.54**	**0.52**	**0.45**

X_{Wo} = Ca/(Ca+Mg+Fe^T); X_{En}= Mg/(Ca+Mg+Fe^T); X_{Fs} = Fe^T/(Ca+Mg+Fe^T); X_{Mg} = Mg/(Fe^{2+}+Mg); bdl = Below Detection Limt

Table 5.5 contd.

Sample No.	D-8									
Domain	7	23	24	31	32	33	34	35	36	37
SiO_2	51.95	51.84	51.93	51.92	51.95	52.02	52.43	51.79	51.80	51.46
TiO_2	0.16	0.15	0.11	0.10	0.15	0.08	0.05	0.08	0.14	0.12
Al_2O_3	1.14	1.26	1.32	1.14	1.15	1.49	1.27	1.66	1.26	1.38
Cr_2O_3	0.09	0.02	bdl	bdl	bdl	bdl	bdl	0.01	0.02	bdl
FeO	14.01	12.83	11.85	12.52	12.88	13.27	11.98	13.51	12.79	12.94
MnO	0.53	0.58	0.37	0.46	0.53	0.35	0.38	0.49	0.49	0.56
MgO	11.29	11.32	11.46	11.55	11.29	11.46	11.59	11.44	11.74	11.56
CaO	20.19	21.82	21.31	21.78	21.46	21.13	21.32	20.86	21.38	21.65
Na_2O	0.39	0.39	0.39	0.33	0.35	0.37	0.30	0.29	0.28	0.28
Total	**99.75**	**100.21**	**98.74**	**99.80**	**99.81**	**100.19**	**99.32**	**100.13**	**99.90**	**99.95**
Si	1.982	1.96	1.99	1.971	1.976	1.969	1.997	1.964	1.96	1.95
Ti	0.005	0	0	0.003	0.004	0.002	0.001	0.002	0	0
Al	0.051	0.06	0.06	0.051	0.052	0.066	0.057	0.074	0.06	0.06
Cr	0.003	bdl	bdl	bdl	bdl	bdl	bdl	bdl	bdl	bdl
Fe^{+3}	0.003	0.04	bdl	0.026	0.013	0.018	bdl	0.015	0.03	0.05
Fe^{+2}	0.444	0.37	0.38	0.371	0.397	0.402	0.382	0.414	0.38	0.36
Mn	0.017	0.02	0.01	0.015	0.017	0.011	0.012	0.016	0.02	0.02
Mg	0.642	0.64	0.65	0.653	0.64	0.647	0.658	0.647	0.66	0.65
Ca	0.825	0.88	0.87	0.886	0.875	0.857	0.870	0.847	0.87	0.88
Na	0.029	0.03	0.03	0.024	0.026	0.027	0.022	0.021	0.02	0.02
Total	4	4	4	4	4	4	4	4	4	4
End member										
X_{Wo}	43.1	45.9	45.8	45.7	45.4	44.6	45.6	44.1	44.8	45.3
X_{En}	33.5	33.1	34.3	33.8	33.3	33.6	34.5	33.6	34.3	33.6
X_{Fs}	23.4	21.1	19.9	20.5	21.3	21.8	20.0	22.3	20.9	21.1
X_{Mg}	**0.61**	**0.61**	**0.63**	**0.62**	**0.61**	**0.61**	**0.63**	**0.60**	**0.62**	**0.61**

X_{Wo} = Ca/(Ca+Mg+Fe^T); X_{En}= Mg/(Ca+Mg+Fe^T); X_{Fs} = Fe^T/(Ca+Mg+Fe^T); X_{Mg} = Mg/(Fe^{2+}+Mg); bdl = Below Detection Limt

Table 5.6 Chemical analysis and structural formulae (on the basis of 18 Oxygen) of Cordierite from high-grade gneisses.

Sample	R-91-97					R-91-96					
Domain	20 (C)	21 (C)	136 (R)	140 (R)	139 (R)	24	25	120	139	13	33
SiO_2	49.69	49.19	48.62	48.76	48.33	48.94	49.24	48.70	49.54	48.56	48.06
Al_2O_3	29.82	29.24	30.62	30.38	30.38	30.11	30.46	30.22	30.38	29.86	29.82
FeO	4.54	5.17	6.03	5.69	5.34	5.87	5.56	6.24	5.33	4.96	5.62
MnO	bdl	bdl	bdl	bdl	bdl	bdl	bdl	bdl	bdl	bdl	bdl
MgO	10.62	10.61	10.16	10.32	10.17	10.20	10.02	9.93	10.17	10.55	10.55
CaO	bdl	bdl	bdl	bdl	bdl	bdl	bdl	bdl	bdl	bdl	bdl
Na_2O	0.12	0.31	0.14	0.13	0.11	0.16	0.14	0.15	0.10	0.09	0.12
K_2O	bdl	bdl	bdl	bdl	bdl	bdl	bdl	bdl	bdl	bdl	bdl
Total	**94.77**	**94.53**	**95.57**	**95.28**	**94.34**	**95.27**	**95.43**	**95.23**	**95.52**	**94.04**	**94.17**
Si	5.205	5.192	5.097	5.118	5.114	5.140	5.151	5.127	5.169	5.145	5.107
Al	3.682	3.638	3.783	3.758	3.789	3.727	3.755	3.750	3.736	3.729	3.735
ΣZ	8.887	8.830	8.881	8.876	8.903	8.867	8.907	8.876	8.905	8.874	8.842
Fe^{2+}	0.397	0.456	0.528	0.499	0.472	0.515	0.487	0.549	0.465	0.440	0.500
Mn	bdl	bdl	bdl	bdl	bdl	bdl	bdl	bdl	bdl	bdl	bdl
Mg	1.658	1.670	1.588	1.615	1.605	1.598	1.563	1.558	1.582	1.667	1.671
Ca	bdl	bdl	bdl	bdl	bdl	bdl	bdl	bdl	bdl	bdl	bdl
ΣY	2.056	2.126	2.116	2.114	2.077	2.113	2.050	2.107	2.047	2.107	2.170
Na	0.023	0.064	0.028	0.027	0.023	0.032	0.029	0.030	0.021	0.019	0.025
K	bdl	bdl	bdl	bdl	bdl	bdl	bdl	bdl	bdl	bdl	bdl
ΣX	0.023	0.064	0.028	0.027	0.023	0.032	0.029	0.030	0.021	0.019	0.025
Total	10.966	11.021	11.025	11.017	11.003	11.012	10.985	11.014	10.973	11.000	11.038
X_{Mg}	**0.79**	**0.78**	**0.75**	**0.76**	**0.77**	**0.75**	**0.76**	**0.74**	**0.77**	**0.79**	**0.77**

X_{Mg} = Mg/(Fe^{2+}+Mg); C = Core; R = Rim; bdl = Below Detection Limt

Table 5.6 contd. (from Pelitic granulites**)**

Sample	D-3														
Domain	36	37	38	39	40	41	42	43	44	45	46	47	48	49	50
SiO_2	49.0	49.35	49.14	49.28	49.46	48.79	49.20	48.53	49.40	48.95	49.15	49.25	48.75	48.19	48.59
Al_2O_3	32.09	32.15	32.46	32.41	32.14	31.65	32.42	32.29	32.47	32.10	32.57	32.38	32.31	31.71	32.03
FeO	7.82	7.78	8.04	7.96	8.03	7.69	8.29	7.26	8.61	8.62	7.95	7.39	7.48	7.53	7.61
MnO	0.08	0.16	0.09	0.06	0.06	0.08	bdl	0.05	0.12	Bdl	0.11	0.03	0.05	0.04	bdl
MgO	8.56	8.68	8.57	8.51	8.74	8.73	8.79	8.79	8.33	8.21	9.08	9.05	8.94	8.93	9.25
CaO	0.01	0.01	0.02	0.03	bdl	0.05	0.01	0.03	0.03	Bdl	0.01	0.02	bdl	bdl	bdl
Na_2O	0.13	0.13	0.12	0.10	0.12	0.11	0.09	0.12	0.10	0.14	0.15	0.13	0.10	0.16	0.12
K_2O	0.01	bdl	0.01	bdl	bdl	bdl	bdl	0.01	bdl	0.02	0.02	bdl	bdl	bdl	bdl
Total	**97.68**	**98.26**	**98.45**	**98.36**	**98.54**	**97.09**	**98.80**	**97.08**	**99.05**	**98.03**	**99.03**	**98.25**	**97.63**	**96.56**	**97.60**
Si	5.062	5.069	5.043	5.058	5.069	5.070	5.036	5.035	5.051	5.057	5.018	5.049	5.033	5.036	5.024
Al	3.908	3.892	3.926	3.920	3.882	3.877	3.911	3.948	3.912	3.908	3.919	3.912	3.932	3.905	3.903
ΣZ	8.970	8.961	8.970	8.978	8.951	8.947	8.947	8.982	8.963	8.965	8.936	8.962	8.965	8.941	8.927
Fe^{2+}	0.676	0.668	0.690	0.683	0.688	0.668	0.709	0.630	0.736	0.745	0.679	0.633	0.646	0.658	0.658
Mn	0.007	0.014	0.008	0.005	0.005	0.007	bdl	0.004	0.011	Bdl	0.010	0.002	0.004	0.003	bdl
Mg	1.318	1.328	1.312	1.302	1.335	1.352	1.341	1.359	1.270	1.264	1.381	1.383	1.376	1.390	1.427
Ca	0.001	0.001	0.002	0.003	bdl	0.005	0.001	0.003	0.003	Bdl	0.001	0.003	bdl	bdl	bdl
ΣY	2.001	2.012	2.011	1.994	2.028	2.032	2.052	1.997	2.020	2.009	2.071	2.020	2.026	2.052	2.084
Na	0.025	0.025	0.024	0.021	0.023	0.023	0.019	0.024	0.019	0.028	0.029	0.025	0.020	0.032	0.025
K	0.001	bdl	0.001	bdl	bdl	bdl	bdl	0.001	bdl	0.002	0.003	bdl	bdl	bdl	bdl
ΣX	0.027	0.025	0.025	0.021	0.023	0.023	0.019	0.024	0.019	0.030	0.032	0.025	0.020	0.032	0.025
Total	10.997	10.998	11.006	10.993	11.002	11.002	11.017	11.004	11.002	11.004	11.039	11.007	11.011	11.026	11.036
X_{Mg}	**0.66**	**0.67**	**0.66**	**0.66**	**0.66**	**0.67**	**0.65**	**0.68**	**0.63**	**0.63**	**0.67**	**0.69**	**0.68**	**0.68**	**0.68**

X_{Mg} = Mg/(Fe^{2+}+Mg); bdl = Below Detection Limt

Table 5.7 Chemical analysis and structural formulae (on the basis of 22 Oxygen) of biotite from high-grade gneisses.

Sample	R-91-97						R-91-96					
Domain	**157**	**160**	**161**	**162**	**122 / 146**	**159**	**63**	**52**	**64**	**58**	**50**	**51**
SiO_2	39.73	39.22	38.27	38.77	40.42	39.07	38.78	38.38	37.88	38.57	38.25	38.94
TiO_2	1.64	1.83	2.08	1.87	1.98	1.68	1.71	1.74	1.62	1.99	1.26	1.14
Al_2O_3	14.07	13.71	14.38	14.61	15.38	14.37	14.97	14.97	14.48	14.57	15.27	15.12
FeO	12.21	12.86	12.02	12.38	12.1	13.07	12.71	11.62	12.41	12.04	12.45	11.49
MgO	18.49	18.15	18.05	17.78	17.66	18.11	17.50	17.71	17.21	17.51	17.26	18.62
CaO	0.05	0.01	0.01	0.02	bdl	0.03	bdl	Bdl	bdl	bdl	bdl	bdl
BaO	0.21	0.1	0.21	0.1	0.42	0.24	bdl	Bdl	0.10	bdl	0.1	0.1
Na_2O	0.72	0.56	0.59	0.65	0.71	0.51	0.64	0.63	0.62	0.67	0.66	0.61
K2O	9.01	9.11	8.85	8.94	8.82	8.02	8.98	8.80	9.16	8.97	9.17	9.08
Cl	0.09	0.04	0.04	0.06	0.05	0.06	0.04	Bdl	0.05	0.05	0.044	0.051
F	1.68	2.24	2.22	2.02	0.51	1.70	2.11	1.78	2.05	2.12	2.29	1.76
Total	**97.91**	**97.82**	**96.7**	**97.2**	**98.05**	**96.85**	**97.44**	**95.77**	**95.60**	**96.50**	**96.61**	**96.75**
Si	5.78	5.76	5.67	5.71	5.66	5.738	5.699	5.698	5.694	5.715	5.685	5.709
Al^{IV}	2.22	2.24	2.33	2.29	2.34	2.262	2.301	2.302	2.306	2.285	2.315	2.291
ΣZ	8	8	8	8	8	8	8	8	8	8	8	8
Al^{VI}	0.19	0.14	0.19	0.24	0.28	0.226	0.292	0.318	0.259	0.259	0.36	0.321
Ti	0.18	0.2	0.23	0.21	0.2	0.185	0.189	0.194	0.184	0.222	0.141	0.126
Fe^{2+}	1.49	1.58	1.49	1.52	1.42	1.606	1.562	1.443	1.559	1.492	1.547	1.409
Ba	0.01	0.01	0.01	0.01	0.02	0.014	bdl	Bdl	0.006	bdl	0.006	0.006
Mg	4.01	3.98	3.99	3.9	4	3.966	3.835	3.921	3.857	3.867	3.824	4.07
ΣX	5.88	5.91	5.91	5.88	5.92	5.997	5.878	5.875	5.865	5.84	5.88	5.93
Ca	0.01	0.01	bdl	0.01	bdl	0.004	bdl	Bdl	bdl	0.001	bdl	bdl
Na	0.2	0.16	0.17	0.19	0.19	0.146	0.181	0.18	0.18	0.192	0.19	0.172
K	1.67	1.71	1.67	1.68	1.57	1.503	1.684	1.666	1.756	1.695	1.739	1.698
ΣY	1.88	1.87	1.84	1.87	1.77	1.653	1.865	1.846	1.936	1.888	1.929	1.87
Cl	0.02	bdl	0.01	0.01	0.01	0.014	0.01	Bdl	0.013	0.012	0.01	0.01
F	0.77	1.04	1.04	0.94	0.22	0.788	0.982	0.833	0.975	0.994	1.076	0.817
$\mathbf{X_{Mg}}$	**0.73**	**0.72**	**0.73**	**0.72**	**0.74**	**0.71**	**0.71**	**0.73**	**0.71**	**0.72**	**0.71**	**0.74**

X_{Mg} = Mg/(Fe^{2+}+Mg); bdl = Below Detection Limt

Table 5.7 contd. (from mafic granulites**)**

Sample	D-8										
Domain	51	52	53	54	57	58	59	60	61	62	63
SiO_2	35.87	34.98	35.02	35.56	35.59	35.95	35.97	35.83	35.46	35.23	35.77
TiO_2	5.89	5.08	5.71	5.47	5.30	5.03	5.32	5.49	5.44	5.28	5.30
Al_2O_3	13.65	13.46	13.57	13.47	13.63	13.74	13.53	13.26	13.48	13.73	13.93
Cr_2O_3	0.09	0.04	0.02	0.21	0.11	0.20	0.18	0.09	0.05	0.08	0.13
FeO	19.68	19.98	21.74	20.74	20.58	20.19	20.90	20.53	20.51	20.25	20.44
MnO	0.08	0.12	0.04	0.11	0.12	0.03	0.07	0.07	0.16	0.07	0.10
MgO	10.45	10.39	10.46	9.91	9.99	10.49	10.31	9.65	10.11	10.43	9.96
CaO	0.06	0.11	0.01	0.01	0.03	0.04	0.04	0.04	0.03	0.03	0.06
Na_2O	0.11	0.56	0.10	0.21	0.09	0.07	0.09	0.23	0.21	0.16	0.39
K_2O	9.53	9.24	9.24	9.11	9.38	9.27	9.26	9.26	9.40	9.37	9.26
Cl	0.67	0.54	0.43	0.41	0.33	0.33	0.39	0.54	0.58	0.56	0.50
F	0.17	0.54	0.20	0.22	0.23	0.21	0.19	0.22	0.16	0.20	0.37
Total	**96.25**	**95.04**	**96.54**	**95.43**	**95.38**	**95.55**	**96.25**	**95.21**	**95.59**	**95.39**	**96.21**
Si	5.489	5.467	5.395	5.510	5.515	5.537	5.520	5.563	5.491	5.460	5.500
Al^{iv}	2.462	2.479	2.464	2.460	2.485	2.463	2.447	2.426	2.460	2.508	2.500
ΣZ	7.951	7.947	7.858	7.969	8.000	8.000	7.968	7.989	7.951	7.968	8.000
Cr	0.011	0.005	0.002	0.026	0.013	0.024	0.022	0.011	0.006	0.010	0.016
Al^{vi}	bdl	bdl	bdl	bdl	0.005	0.031	bdl	bdl	bdl	bdl	0.024
Ti	0.678	0.597	0.662	0.637	0.618	0.583	0.614	0.641	0.634	0.615	0.613
Fe^{+2}	2.518	2.611	2.800	2.687	2.667	2.600	2.682	2.665	2.656	2.624	2.628
Mn	0.010	0.016	0.005	0.014	0.016	0.004	0.009	0.009	0.021	0.009	0.013
Mg	2.384	2.421	2.402	2.289	2.308	2.409	2.359	2.233	2.334	2.410	2.283
ΣX	5.602	5.650	5.872	5.654	5.627	5.651	5.686	5.560	5.650	5.669	5.576
Ca	0.010	0.018	0.002	0.002	0.005	0.007	0.007	0.007	0.005	0.005	0.010
Na	0.033	0.170	0.030	0.063	0.027	0.021	0.027	0.069	0.063	0.048	0.116
K	1.860	1.842	1.816	1.800	1.854	1.821	1.813	1.834	1.857	1.852	1.816
ΣY	1.903	2.030	1.847	1.865	1.886	1.849	1.846	1.910	1.925	1.905	1.942
Cl	0.174	0.143	0.112	0.108	0.087	0.086	0.101	0.142	0.152	0.147	0.130
F	0.082	0.267	0.097	0.108	0.113	0.102	0.092	0.108	0.078	0.098	0.180
X_{Mg}	**0.49**	**0.48**	**0.46**	**0.46**	**0.46**	**0.48**	**0.47**	**0.46**	**0.47**	**0.48**	**0.46**

X_{Mg} = Mg/(Fe^{2+}+Mg); bdl = Below Detection Limt

Table 5.7 contd. (from mafic and pelitic granulites**)**

	Mafic granulite					Pelitic granulites					
Sample	**K-1**					**D-3**					
Domain	30	37	51	52	53	21	22	24	26	29	34
SiO_2	36.24	36.37	35.98	35.75	36.52	36.92	36.87	36.79	36.98	36.64	36.43
TiO_2	5.43	5.62	5.55	5.37	5.39	1.78	1.99	1.55	1.93	1.82	1.72
Al_2O_3	13.69	13.96	13.74	13.67	13.84	16.37	16.01	16.56	16.5	16.12	16.34
Cr_2O_3	0.27	0.18	0.19	0.25	0.17	bdl	bdl	0.02	bdl	bdl	0.07
FeO	19.34	17.64	18.91	19.58	18.61	15.84	15.34	15.9	16.4	16.61	16.65
MnO	bdl	bdl	0.09	0.09	0.05	bdl	0.06	0	0.17	0.02	0
MgO	11.75	11.85	11.94	11.62	11.55	13.82	13.58	13.56	13.98	13.04	12.94
CaO	0.01	0.02	0.01	0.07	bdl	0.02	bdl	bdl	0.02	bdl	0.03
Na_2O	bdl	bdl	bdl	bdl	bdl	0.53	0.53	0.42	0.58	0.48	0.59
K_2O	9.25	9.24	9.19	9.31	9.56	8.35	8.48	8.38	8.63	8.41	8.49
Cl	0.13	0.11	0.15	0.13	0.16	0.05	0.05	0.03	0.03	0.05	0.03
F	0.26	0.34	0.23	0.21	0.31	1.38	1.34	1.63	1.37	1.31	1.47
Total	**96.37**	**95.33**	**95.98**	**96.05**	**96.16**	**95.05**	**94.25**	**94.84**	**96.58**	**94.51**	**94.77**
Si	5.503	5.537	5.48	5.46	5.55	5.59	5.63	5.6	5.54	5.61	5.58
Al^{iv}	2.45	2.463	2.47	2.46	2.45	2.41	2.37	2.4	2.46	2.39	2.42
ΣZ	7.953	8	7.94	7.93	8	8	8	8	8	8	8
Cr	0.032	0.022	0.02	0.03	0.02	bdl	bdl	0.003	bdl	0.52	0.53
Al^{vi}	bdl	0.042	bdl	bdl	0.02	0.52	0.51	0.57	0.45	0.21	0.2
Ti	0.62	0.644	0.64	0.62	0.62	0.2	0.23	0.18	0.22	bdl	0.008
Fe^{+2}	2.456	2.246	2.41	2.5	2.36	2.01	1.96	2.02	2.05	2.13	2.13
Mn	bdl	bdl	0.01	0.01	0.01	bdl	0.008	bdl	0.022	0.003	bdl
Mg	2.66	2.689	2.71	2.65	2.61	3.12	3.09	3.08	3.12	2.98	2.95
ΣX	5.768	5.643	5.79	5.81	5.64	5.85	5.79	5.85	5.87	5.83	5.82
Ca	0.002	0.003	bdl	0.01	bdl	0.002	bdl	bdl	0.002	bdl	0.005
Na	bdl	bdl	bdl	bdl	bdl	0.16	0.16	0.12	0.17	0.14	0.18
K	1.792	1.794	1.78	1.82	1.85	1.61	1.65	1.63	1.65	1.64	1.66
ΣY	1.794	1.797	1.79	1.83	1.85	1.77	1.81	1.75	1.82	1.78	1.84
Cl	0.033	0.028	0.04	0.03	0.04	0.013	0.012	0.007	0.007	0.012	0.009
F	0.125	0.164	0.11	0.1	0.15	0.66	0.65	0.78	0.65	0.64	0.71
X_{Mg}	**0.52**	**0.54**	**0.53**	**0.51**	**0.53**	**0.61**	**0.61**	**0.60**	**0.60**	**0.58**	**0.58**

X_{Mg} = Mg/(Fe^{2+}+Mg); bdl = Below Detection Limt

Table 5.8 Chemical analysis and structural formulae (on the basis of 32 Oxygen) of Plagioclase from mafic granulites.

Sample	**D-8**									
Domain	6	20	21	22	23	24	25	26	27	28
SiO_2	57.37	55.98	55.97	57.70	56.91	57.31	57.53	56.63	55.99	57.41
Al_2O_3	26.73	26.96	27.19	26.77	26.76	26.98	26.86	26.91	26.97	26.79
FeO	0.05	bdl	bdl	bdl	bdl	bdl	bdl	bdl	bdl	bdl
CaO	8.99	9.57	9.91	9.34	9.43	8.88	9.39	9.72	9.99	9.68
Na_2O	6.15	6.38	5.99	6.23	5.97	6.22	6.11	5.86	5.99	6.27
K_2O	0.29	0.17	0.18	0.19	0.19	0.16	0.16	0.19	0.16	0.18
Total	**99.58**	**99.06**	**99.24**	**100.23**	**99.26**	**99.55**	**100.05**	**99.31**	**99.10**	**100.33**
Si	10.325	10.169	10.145	10.321	10.281	10.305	10.306	10.236	10.165	10.278
Al	5.669	5.771	5.808	5.643	5.697	5.717	5.671	5.732	5.770	5.652
Fe^{+2}	0.008	bdl	bdl	bdl	bdl	bdl	bdl	bdl	bdl	bdl
Ca	1.733	1.862	1.924	1.790	1.825	1.711	1.802	1.882	1.943	1.857
Na	2.146	2.247	2.105	2.161	2.091	2.168	2.122	2.053	2.108	2.176
K	0.067	0.039	0.042	0.043	0.044	0.037	0.037	0.044	0.037	0.041
Total	19.947	20.089	20.024	19.959	19.938	19.938	19.938	19.947	20.023	20.004
An	43.9	44.89	47.3	44.8	46.1	43.7	45.5	47.3	47.5	45.6
Ab	54.4	54.2	51.7	54.1	52.8	55.4	53.6	51.6	51.6	53.4
Or	1.7	1.0	1.0	1.1	1.1	0.9	0.9	1.1	0.9	1.0

Table 5.8 contd.

Sample	K-1									
Domain	6	7	8	31	32	61	62	63	64	65
SiO_2	55.83	55.36	54.76	52.22	54.92	53.82	52.59	54.86	55.71	55.62
Al_2O_3	28.17	28.47	28.76	29.99	28.91	28.89	29.95	27.88	27.83	28.24
FeO	bdl	0.10	0.11	0.10	0.13	0.10	0.10	0.05	0.05	0.13
CaO	10.10	10.90	11.69	13.63	10.81	11.88	13.44	11.39	10.76	11.34
Na_2O	5.45	5.01	4.69	3.67	5.12	4.56	3.44	4.78	5.14	4.65
K_2O	0.09	0.17	0.13	0.09	0.12	0.12	0.12	0.17	0.13	0.17
Total	**99.64**	**100.01**	**100.14**	**99.70**	**100.01**	**99.37**	**99.64**	**99.13**	**99.62**	**100.15**
Si	10.058	9.965	9.866	9.508	9.891	9.784	9.561	9.975	10.058	9.997
Al	5.981	6.039	6.107	6.435	6.136	6.190	6.417	5.974	5.921	5.982
Fe^{+2}	bdl	0.015	0.017	0.015	0.020	0.015	0.015	0.008	0.008	0.020
Ca	1.949	2.102	2.256	2.659	2.086	2.314	2.618	2.219	2.081	2.184
Na	1.904	1.748	1.638	1.295	1.788	1.607	1.212	1.685	1.799	1.620
K	0.021	0.039	0.030	0.021	0.028	0.028	0.028	0.039	0.030	0.039
Total	19.913	19.909	19.914	19.933	19.948	19.938	19.851	19.900	19.896	19.842
An	50.3	54.0	57.5	66.9	53.5	58.6	67.9	56.3	53.2	56.8
Ab	49.1	45.0	41.7	32.6	45.8	40.7	31.4	42.7	46.0	42.2
Or	0.5	1.0	0.8	0.5	0.7	0.7	0.7	1.0	0.8	1.0

bdl = Below Detection Limt

Table 5.8 contd. [from mafic (RP-1) and pelitic granulites (D-3)**]**

Sample	RP-1							D-3			
Domain	111	112	113	114	115	116	117	77	78	79	80
SiO_2	57.83	57.39	57.96	58.28	56.84	57.41	57.69	59.12	59.28	59.49	58.59
Al_2O_3	25.94	26.34	26.13	26.05	26.63	26.23	26.63	25.43	25.46	25.61	25.32
FeO	0.01	0.08	0.06	0.07	0.16	0.06	bdl	bdl	bdl	0.13	0.05
CaO	8.93	9.33	8.65	8.34	9.62	8.85	8.80	7.66	7.75	7.8	7.76
Na_2O	6.45	6.34	6.47	6.37	5.98	6.47	5.97	6.85	6.8	6.8	6.86
K_2O	0.35	0.25	0.33	0.27	0.26	0.29	0.37	0.16	0.16	0.05	0.15
Total	**99.51**	**99.73**	**99.60**	**99.38**	**99.49**	**99.31**	**99.46**	**99.21**	**99.45**	**99.89**	**98.72**
Si	10.422	10.334	10.425	10.480	10.267	10.369	10.377	10.62	10.62	10.61	10.59
Al	5.509	5.590	5.539	5.521	5.669	5.583	5.645	5.38	5.38	5.39	5.39
Fe^{+2}	0.002	0.012	0.009	0.011	0.024	0.009	bdl	bdl	bdl	0.02	0.01
Ca	1.724	1.800	1.667	1.607	1.862	1.712	1.696	1.47	1.49	1.49	1.5
Na	2.253	2.213	2.256	2.221	2.094	2.265	2.082	2.38	2.36	2.35	2.4
K	0.080	0.057	0.076	0.062	0.060	0.067	0.085	0.04	0.04	0.01	0.03
Total	19.991	20.006	19.971	19.901	19.976	20.006	19.884	19.9	19.89	19.88	19.93
An	42.5	44.2	41.7	41.3	46.4	42.3	43.9	37.8	38.3	38.7	38.1
Ab	55.5	54.4	56.4	57.1	52.2	56.0	53.9	61.2	60.8	61.0	61.0
Or	2.0	1.4	1.9	1.6	1.5	1.7	2.2	0.9	0.9	0.3	0.9

bdl = Below Detection Limt

Table 5.9 Chemical analysis and structural formulae (on the basis of 10 Oxygen) of Sillimanite from pelitic granulites.

Sample	**D-3**									
Domain	7	8	9	10	11	12	13	14	15	16
SiO_2	37.58	38.21	37.84	37.05	37.16	38.12	37.89	37.27	38.16	38.23
TiO_2	bdl	bdl	bdl	bdl	bdl	bdl	bdl	bdl	bdl	bdl
Al_2O_3	62.15	61.25	61.1	61.48	62.18	61.52	61.84	62.11	62.27	61.64
Cr_2O_3	0.032	0.026	0.031	0.029	0.018	0.024	0.017	0.034	0.045	0.041
FeO	0.52	0.58	0.51	0.57	0.48	0.47	0.42	0.59	0.67	0.39
Total	100.28	100.07	99.48	99.13	99.84	100.13	100.17	100.00	101.15	100.30
Si	2.026	2.063	2.055	2.021	2.012	2.056	2.043	2.016	2.041	2.058
Ti	bdl	bdl	bdl	bdl	bdl	bdl	bdl	bdl	bdl	bdl
Al	3.948	3.897	3.910	3.953	3.968	3.910	3.929	3.959	3.924	3.910
Cr	0.001	0.001	0.001	0.001	0.001	0.001	0.001	0.001	0.002	0.002
Fe	0.023	0.026	0.023	0.026	0.022	0.021	0.019	0.027	0.030	0.018
Total	5.999	5.988	5.989	6.002	6.003	5.988	5.992	6.004	5.996	5.987

bdl = Below Detection Limt

Table 5.10 Chemical analysis and structural formulae (on the basis of 28 Oxygen) of Chlorite from high-grade gneisses (R-91-97).

	R-91-96				**R-91-97**					
Domain	53	54	55	56	96	97	98	99	100	156
SiO_2	44.75	45.26	47.55	45.95	44.11	45.05	40.36	39.91	41.67	39.27
Al_2O_3	10.64	11.27	8.26	10.80	24.45	23.09	21.50	21.18	24.90	21.11
Fe_2O_3	9.21	9.30	10.61	9.76	13.08	12.20	15.94	15.85	12.98	8.56
FeO	13.44	12.81	11.72	12.07	bdl	bdl	1.79	1.79	bdl	9.36
MgO	15.46	15.55	16.14	16.07	5.21	5.13	5.46	5.36	4.90	12.48
CaO	0.06	0.06	0.02	0.03	1.14	1.11	1.04	1.06	1.16	0.14
Na_2O	1.31	1.67	1.15	1.47	0.18	0.35	0.11	0.10	0.20	0.08
K_2O	0.08	bdl	bdl	bdl	0.88	0.89	0.59	0.50	0.83	0.10
BaO	bdl	bdl	bdl	bdl	0.38	0.24	0.17	0.34	0.28	bdl
F	0.30	0.39	0.27	0.36	bdl	bdl	bdl	bdl	bdl	bdl
Cl	0.020	bdl	bdl	bdl	0.064	0.204	0.060	0.081	0.052	0.045
Total	**95.272**	**96.312**	**95.719**	**96.502**	**89.489**	**88.270**	**87.031**	**86.164**	**86.972**	**91.153**
Si	7.997	7.951	8.392	8.037	7.871	8.097	7.604	7.608	7.666	7.632
Al^{iv}	0.003	0.049	bdl	bdl	0.129	bdl	0.396	0.392	0.334	0.368
ΣZ	8	8	8.392	8.037	8	8.097	8	8	8	8
Al^{vi}	2.316	2.372	1.780	2.308	5.207	5.076	4.597	4.586	5.273	3.714
Fe^{3+}	1.239	1.230	1.409	1.284	1.756	1.650	2.260	2.273	1.797	1.284
Fe^{+2}	2.009	1.882	1.730	1.765	bdl	bdl	0.283	0.286	bdl	1.561
Mg	4.118	4.072	4.246	4.190	1.384	1.374	1.533	1.523	1.344	3.708
Ca	0.011	0.011	0.003	0.006	0.218	0.215	0.210	0.217	0.229	0.030
Na	0.908	1.138	0.787	0.997	0.125	0.244	0.083	0.074	0.143	0.062
K	0.036	bdl	bdl	bdl	0.401	0.408	0.284	0.241	0.390	0.051
Ba	bdl	bdl	bdl	bdl	0.053	0.034	0.025	0.051	0.040	bdl
F	0.339	0.433	0.301	0.398	bdl	bdl	bdl	bdl	bdl	bdl
Cl	0.012	bdl	bdl	bdl	0.039	0.124	0.038	0.052	0.032	0.030
X_{Mg}	**0.56**	**0.57**	**0.57**	**0.58**	**0.44**	**0.45**	**0.38**	**0.37**	**0.43**	**0.57**

X_{Mg} = Mg/(Fe^{2+}+Mg); bdl = Below Detection Limt

Table 5.11 Chemical analysis and structural formulae (on the basis of 4 Oxygen) of Ilmenite from high-grade gneisses.

Sample	R-91-97					R-91-96					
Domain	9	10	27	28	32	34	35	36	37	38	41
TiO_2	49.32	47.64	47.86	49.91	46.99	50.50	49.20	48.39	47.71	46.98	48.82
Cr_2O_3	0.03	0.04	bdl	bdl	bdl	0.01	bdl	0.01	0.02	bdl	bdl
Al_2O_3	bdl	bdl	bdl	bdl	1.77	bdl	bdl	bdl	0.04	bdl	bdl
FeO	48.57	47.57	47.01	46.92	45.10	45.14	46.99	46.89	47.05	48.66	46.96
MnO	0.19	0.24	0.15	0.06	0.07	0.01	0.06	0.03	0.11	0.01	0.17
MgO	0.05	0.05	0.07	0.06	0.06	0.73	0.05	0.13	0.55	0.08	0.05
CaO	bdl	0.01	bdl	0.02	0.02	bdl	0.01	bdl	0.03	0.01	bdl
SiO_2	0.01	0.12	0.01	0.06	0.25	0.13	0.02	0.14	1.32	0.04	0.05
TOTAL	**98.17**	**95.66**	**95.10**	**97.04**	**94.26**	**96.52**	**96.34**	**95.59**	**96.82**	**95.79**	**96.05**
Ti	1.934	1.923	1.936	1.967	1.898	1.985	1.957	1.946	1.920	1.901	1.951
Cr	0.001	0.002	bdl	bdl	bdl	bdl	bdl	bdl	0.001	bdl	bdl
Al	bdl	bdl	bdl	bdl	0.112	bdl	bdl	bdl	0.002	bdl	bdl
Fe^{3+}	0.125	0.124	0.135	0.115	0.154	0.106	0.123	0.128	0.106	0.136	0.128
Fe^{+2}	2.117	2.135	2.115	2.056	2.026	1.973	2.078	2.096	2.105	2.189	2.086
Mn	0.009	0.011	0.007	0.003	0.003	bdl	0.003	0.001	0.005	bdl	0.008
Mg	0.004	0.004	0.006	0.005	0.005	0.057	0.004	0.011	0.044	0.006	0.004
Ca	bdl	0.001	bdl	0.001	0.001	bdl	0.001	bdl	0.002	bdl	bdl
Si	bdl	0.006	bdl	0.003	0.013	0.007	0.001	0.007	0.071	0.002	0.002
Total	4.065	4.076	4.064	4.033	4.046	4.015	4.043	4.054	4.078	4.098	4.049

bdl = Below Detection Limt

Table 5.11 contd. (from mafic granulites)

Sample	**RP-1**			**D-8**				**K-1**		
Domain	67	70	71	80	84	11	12	33	79	80
TiO_2	51.43	51	52.22	52.48	52.48	51.63	52	52.01	52.17	52.02
Cr_2O_3	0.14	0.16	0.12	0.12	0.17	0.21	0.19	0.18	0.17	0.17
Al_2O_3	0.5	0.58	0.61	0.56	0.57	0.53	0.68	0.46	0.35	0.43
FeO	47.34	46.53	46.77	46.13	45.47	46.35	46.01	47.18	47.14	47.25
MnO	1.34	0.88	1.02	1.36	1.29	0.66	0.58	0.55	0.51	0.73
MgO	0.1	0.02	bdl	0.03	bdl	0.39	0.42	0.41	0.45	0.25
CaO	0.08	0.07	0.06	0.05	0.06	0.07	0.1	0.03	0.04	0.07
Total	**100.93**	**99.24**	**100.8**	**100.73**	**100.04**	**99.84**	**99.98**	**100.82**	**100.83**	**100.92**
Ti	1.944	1.956	1.967	1.98	1.98	1.966	1.973	1.964	1.97	1.96
Cr	0.006	0.006	0.005	0.005	0.01	0.008	0.008	0.007	0.01	0.01
Al	0.03	0.035	0.036	0.03	0.03	0.012	0.016	0.01	0.01	0.01
Fe^{3+}	0.014	0.024	0.016	0.018	0.021	0.021	0.008	0.009	0.012	0.014
Fe^{+2}	1.99	1.984	1.959	1.93	1.91	1.963	1.941	1.98	1.98	1.98
Mn	0.057	0.038	0.043	0.06	0.05	0.028	0.025	0.023	0.02	0.03
Mg	0.007	0.002	bdl	bdl	bdl	0.029	0.032	0.031	0.03	0.02
Ca	0.004	0.004	0.003	0.003	0.003	0.004	0.005	0.002	0.002	0.004
Total	4.038	4.024	4.013	4.01	4	4.011	4	4.017	4.02	4.02

bdl = Below Detection Limt